*IMA Journal of Numerical Analysis* (2024) **44**, 654–679
https://doi.org/10.1093/imanum/drad025
Advance Access publication on 22 May 2023

# Improved uniform error bounds on time-splitting methods for the long-time dynamics of the weakly nonlinear Dirac equation

Weizhu Bao
*Department of Mathematics, National University of Singapore, Singapore 119076, Singapore*
matbaowz@nus.edu.sg

Yongyong Cai*
*Laboratory of Mathematics and Complex Systems and School of Mathematical Sciences, Beijing Normal University, Beijing 100875, China*
*Corresponding author: yongyong.cai@bnu.edu.cn

and

Yue Feng
*Department of Mathematics, National University of Singapore, Singapore 119076, Singapore*

[Received on 11 March 2022; revised on 14 November 2022]

Improved uniform error bounds on time-splitting methods are rigorously proven for the long-time dynamics of the weakly nonlinear Dirac equation (NLDE), where the nonlinearity strength is characterized by a dimensionless parameter $\varepsilon \in (0, 1]$. We adopt a second-order Strang splitting method to discretize the NLDE in time, and combine with the Fourier pseudospectral method in space for the full-discretization. By employing the regularity compensation oscillation (RCO) technique, where the high frequency modes are controlled by the regularity of the exact solution, and the low frequency modes are analyzed by phase cancellation and energy method, we establish improved uniform error bounds at $O(\varepsilon^2\tau^2)$ and $O(h^{m-1} + \varepsilon^2\tau^2)$ for the second-order Strang splitting semidiscretization and full-discretization up to the long-time $T_\varepsilon = T/\varepsilon^2$ with $T > 0$ fixed, respectively. Furthermore, the numerical scheme and error estimates are extended to an oscillatory NLDE, which propagates waves with $O(\varepsilon^2)$ wavelength in time and at $O(\varepsilon^{-2})$ wave speed in space. Finally, numerical examples verifying our analytical results are given.

*Keywords*: nonlinear Dirac equation; long-time dynamics; time-splitting method; improved uniform error bound; regularity compensation oscillation (RCO).

## 1. Introduction

Long-time dynamics of Hamiltonian partial differential equations (PDE) has attracted much interest in recent years from both analytical and numerical aspects (Cazenave & Vazquez, 1986; Faou *et al.*, 2010; Faou & Grébert, 2011; Sasaki, 2015). The change of a small nonlinear perturbation to the dynamics of a linear Hamiltonian PDE deserves careful considerations (Hairer & Lubich, 2008; Gauckler & Lubich, 2010). The nonlinear Dirac equation (NLDE) is widely used in many fields such as the electron self-interaction (Dirac, 1928; Esteban & Séré, 1997), quantum field theory (Thirring, 1958; Soler, 1970), Bose–Einstein condensate (BEC) (Haddad & Carr, 2015) and graphene as well as other 2D materials (Fefferman & Weistein, 2012; Brinkman *et al.*, 2014).

We start with the NLDE in three dimensions (3D) (Dirac, 1928, 1958)

$$i\hbar\partial_t\Psi = \left(-ic\hbar\sum_{j=1}^{3}\alpha_j\partial_j + mc^2\beta\right)\Psi + \mathbf{F}(\Psi)\Psi, \quad \mathbf{x}\in\mathbb{R}^3, \quad t>0. \tag{1.1}$$

Here, $i=\sqrt{-1}$ is the imaginary unit, $t$ is time, $\mathbf{x}=(x_1,x_2,x_3)^T$ is the spatial coordinate vector, $\partial_j$ represents $\partial_{x_j}$ for $j=1,2,3$ and $\Psi:=\Psi(t,\mathbf{x})=(\psi_1(t,\mathbf{x}),\psi_2(t,\mathbf{x}),\psi_3(t,\mathbf{x}),\psi_4(t,\mathbf{x}))^T\in\mathbb{C}^4$ is the complex-valued spinor wave function. The physical constants in (1.1) include the reduced Planck constant $\hbar$, the speed of the light $c$ and the particle's rest mass $m$. In addition, the $4\times4$ matrices $\alpha_1,\alpha_2,\alpha_3$ and $\beta$ are defined as

$$\alpha_1=\begin{pmatrix}\mathbf{0}&\sigma_1\\ \sigma_1&\mathbf{0}\end{pmatrix}, \quad \alpha_2=\begin{pmatrix}\mathbf{0}&\sigma_2\\ \sigma_2&\mathbf{0}\end{pmatrix}, \quad \alpha_3=\begin{pmatrix}\mathbf{0}&\sigma_3\\ \sigma_3&\mathbf{0}\end{pmatrix}, \quad \beta=\begin{pmatrix}I_2&\mathbf{0}\\ \mathbf{0}&-I_2\end{pmatrix}, \tag{1.2}$$

where $\sigma_j$ $(j=1,2,3)$ are the Pauli matrices

$$\sigma_1=\begin{pmatrix}0&1\\1&0\end{pmatrix}, \quad \sigma_2=\begin{pmatrix}0&-i\\ i&0\end{pmatrix}, \quad \sigma_3=\begin{pmatrix}1&0\\0&-1\end{pmatrix}. \tag{1.3}$$

The nonlinearity $\mathbf{F}(\Psi)$ in (1.1) is usually taken as

$$\mathbf{F}(\Psi)=g_1(\Psi^*\beta\Psi)\beta+g_2|\Psi|^2I_4, \tag{1.4}$$

where $g_1,g_2\in\mathbb{R}$ are two parameters, $|\Psi|^2=\Psi^*\Psi$ with $\Psi^*=\overline{\Psi}^T$ the complex conjugate transpose of $\Psi$ and $I_4$ is the $4\times4$ identity matrix. The choice of nonlinearity is motivated from BEC with a chiral confinement and/or spin-orbit coupling, e.g., $g_1=0$ and $g_2\neq0$ (Chang *et al.*, 1975; Haddad & Carr, 2015), and the so-called Soler model in quantum field theory, e.g., $g_2=0$ and $g_1\neq0$ (Thirring, 1958; Soler, 1970; Fushchich & Shtelen, 1983).

To study the dynamics, the initial data is usually assigned as

$$\Psi(t=0,\mathbf{x})=\Psi_0(\mathbf{x}), \quad \mathbf{x}\in\mathbb{R}^3.$$

The NLDE (1.1) is dispersive and time symmetric, and it conserves the total mass as

$$\|\Psi(t,\cdot)\|^2:=\int_{\mathbb{R}^3}|\Psi(t,\mathbf{x})|^2\,\mathrm{d}\mathbf{x}=\int_{\mathbb{R}^3}\sum_{j=1}^{4}|\psi_j(t,\mathbf{x})|^2\,\mathrm{d}\mathbf{x}\equiv\|\Psi(0,\cdot)\|^2=\|\Psi_0\|^2, \quad t>0, \tag{1.5}$$

and the energy as

$$E(t):=\int_{\mathbb{R}^3}\left(-ic\hbar\sum_{j=1}^{3}\Psi^*\alpha_j\partial_j\Psi+mc^2\Psi^*\beta\Psi+H(\Psi)\right)\mathrm{d}\mathbf{x}\equiv E(0), \quad t>0, \tag{1.6}$$

where

$$H(\Psi) = \frac{g_1}{2}\left(\Psi^*\beta\Psi\right)^2 + \frac{g_2}{2}|\Psi|^4, \quad \Psi \in \mathbb{C}^4. \tag{1.7}$$

For the nondimensionalization of the NLDE (1.1), we take

$$\tilde{\mathbf{x}} = \frac{\mathbf{x}}{x_s}, \quad \tilde{t} = \frac{t}{t_s}, \quad \tilde{\Psi}(\tilde{t}, \tilde{\mathbf{x}}) = x_s^{3/2}\Psi(t, \mathbf{x}), \tag{1.8}$$

where the scaling is $L^2$ invariant, and $x_s$ and $t_s$ are the length unit and time unit, respectively. When the interaction energy (of order $g_j x_s^{-3}, j = 1, 2$ ) is significantly less than the kinetic energy (of order $c\hbar/x_s = mc^2$), i.e., $g_j x_s^{-2}/c\hbar = \varepsilon^2$ $(j = 1, 2)$ with the dimensionless parameter $0 < \varepsilon \ll 1$, under the choice in the standard regime as $x_s = \frac{\hbar}{mc}$ and $t_s = \frac{\hbar}{mc^2}$, plugging (1.8) into (1.1), after some simplification and then removing all $\tilde{}$, we obtain the following dimensionless NLDE in 3D

$$i\partial_t\Psi = \left(-i\sum_{j=1}^{3}\alpha_j\partial_j + \beta\right)\Psi + \varepsilon^2\mathbf{F}(\Psi)\Psi, \tag{1.9}$$

where

$$\mathbf{F}(\Psi) = \lambda_1(\Psi^*\beta\Psi)\beta + \lambda_2|\Psi|^2 I_4, \quad \Psi \in \mathbb{C}^4, \tag{1.10}$$

with $\lambda_1, \lambda_2 = O(1)$ two dimensionless constants for the interaction strength. The weakly interacting regime has been adopted to study the BEC of $^{87}$Rb (Haddad & Carr, 2009).

By introducing a re-scaling in time $s = \varepsilon^2 t$ and denoting $\Theta(s, \mathbf{x}) = \Psi(s/\varepsilon^2, \mathbf{x})$, we can reformulate the weakly NLDE (1.9) to an oscillatory NLDE as

$$i\partial_s\Theta(s, \mathbf{x}) = \left(-i\frac{1}{\varepsilon^2}\sum_{j=1}^{3}\alpha_j\partial_j + \frac{1}{\varepsilon^2}\beta\right)\Theta(s, \mathbf{x}) + \mathbf{F}(\Theta(s, \mathbf{x}))\Theta(s, \mathbf{x}), \quad \mathbf{x} \in \mathbb{R}^3, \quad s > 0, \tag{1.11}$$

which is the NLDE in the simultaneously massless and nonrelativistic regime (Bao *et al.*, 2022b), i.e., the mass of the particle is much less than the mass unit and the wave speed is much less than the speed of light. The oscillatory NLDE (1.11) propagates waves with wavelength at $O(\varepsilon^2)$ in time and $O(1)$ in space with the wave speed at $O(\varepsilon^{-2})$. We emphasize that it is quite different from the NLDE in the nonrelativistic regime, where the wave speed is $O(1)$ (Bao *et al.*, 2020). The dynamics of the oscillatory NLDE (1.11) up to the fixed time $T$ is equivalent to the long-time dynamics of the weakly NLDE (1.9) up to the time $T/\varepsilon^2$.

As a common practice, it is desirable to consider (1.11) or (1.9) on a bounded rectangular domain with periodic boundary condition. In one dimension (1D) and two dimensions (2D), the weakly NLDE (1.9) can be simplified to the following NLDE for the two-component wave function $\Phi := \Phi(t, \mathbf{x}) =$

$(\phi_1(t,\mathbf{x}),\phi_2(t,\mathbf{x}))^T \in \mathbb{C}^2$ $(d=1,2)$ as (Bao *et al.*, 2016)

$$i\partial_t \Phi = \left(-i\sum_{j=1}^{d}\sigma_j\partial_j + \sigma_3\right)\Phi + \varepsilon^2\mathbf{F}(\Phi)\Phi, \quad \mathbf{x}\in\Omega\subset\mathbb{R}^d, \tag{1.12}$$

where $\Omega = \prod_{j=1}^{d}(a_j,b_j)\subset\mathbb{R}^d$ is a bounded domain and the periodic boundary condition is imposed, $I_2$ is the $2\times 2$ identity matrix and

$$\mathbf{F}(\Phi) = \lambda_1(\Phi^*\sigma_3\Phi)\sigma_3 + \lambda_2|\Phi|^2 I_2, \quad \Phi\in\mathbb{C}^2. \tag{1.13}$$

The initial data is taken as

$$\Phi(t=0,\mathbf{x}) = \Phi_0(\mathbf{x}), \quad \mathbf{x}\in\overline{\Omega}. \tag{1.14}$$

In addition, the NLDE (1.12) conserves the total mass as

$$\|\Phi(t,\cdot)\|^2 := \int_\Omega |\Phi(t,\mathbf{x})|^2\,\mathrm{d}\mathbf{x} = \int_\Omega \sum_{j=1}^{2}|\phi_j(t,\mathbf{x})|^2\,\mathrm{d}\mathbf{x} \equiv \|\Phi(0,\cdot)\|^2 = \left\|\Phi_0\right\|^2, \quad t\geqslant 0, \tag{1.15}$$

and the energy as

$$E(t) := \int_\Omega \left(-i\sum_{j=1}^{d}\Phi^*\sigma_j\partial_j\Phi + \Phi^*\sigma_3\Phi + \varepsilon^2 G(\Phi)\right)\mathrm{d}\mathbf{x} \equiv E(0), \quad t\geqslant 0, \tag{1.16}$$

where

$$G(\Phi) = \frac{\lambda_1}{2}\left(\Phi^*\sigma_3\Phi\right)^2 + \frac{\lambda_2}{2}|\Phi|^4, \quad \Phi\in\mathbb{C}^2. \tag{1.17}$$

Furthermore, by introducing a new variable $\Upsilon := \Upsilon(t,\mathbf{x}) = \varepsilon\Phi(t,\mathbf{x})$, we can reformulate the weakly NLDE (1.12) with initial data (1.14) into the following NLDE with $O(\varepsilon)$ initial data as

$$\begin{cases} i\partial_t\Upsilon = \left(-i\sum_{j=1}^{d}\sigma_j\partial_j + \sigma_3\right)\Upsilon + \mathbf{F}(\Upsilon)\Upsilon, \quad \mathbf{x}\in\Omega, \quad t>0, \\ \Upsilon(t=0,\mathbf{x}) = \varepsilon\Phi_0(\mathbf{x}). \end{cases} \tag{1.18}$$

The problem with small initial data is widely used in the study on the existence of solutions and long-time dynamics of the nonlinear problem. For convenience of readers, Table 1 shows the properties of the NLDE in different scalings.

For the NLDE (1.12) with $\varepsilon = 1$, i.e., the classical regime, there are extensive analytical and numerical studies in the literature. For the existence and multiplicity of bound states and/or standing wave solutions, we refer to Cazenave & Vazquez (1986), Balabane *et al.* (1988), Fushchich & Zhdanov (1989),

TABLE 1 *Comparison of the NLDE in different scalings*

| | weakly NLDE (1.12) | small data (1.18) | oscillatory (1.11) | nonrelativistic regime (Bao *et al.*, 2017) |
|---|---|---|---|---|
| amplitude | $O(1)$ | $O(\varepsilon)$ | $O(1)$ | $O(1)$ |
| wavelength in space | $O(1)$ | $O(1)$ | $O(1)$ | $O(1)$ |
| wavelength in time | $O(1)$ | $O(1)$ | $O(\varepsilon^2)$ | $O(\varepsilon^2)$ |
| wave velocity | $O(1)$ | $O(1)$ | $O(\varepsilon^{-2})$ | $O(1)$ |
| energy | $O(1)$ | $O(\varepsilon^2)$ | $O(\varepsilon^{-2})$ | $O(\varepsilon^{-2})$ |
| life-span | $O(\varepsilon^{-2})$ | $O(\varepsilon^{-2})$ | $O(1)$ | $O(1)$ |

Esteban & Séré (1997), Pecher (2014), Bartsch & Ding (2006), Komech & Komech (2010) and references therein. For the special case $d = 1$ and $\varepsilon = 1$ in the NLDE (1.12) with $\lambda_1 = -1$ and $\lambda_2 = 0$ in the nonlinearity (1.13), it admits explicit soliton solutions (Rafelski, 1977; Takahashi, 1979; Fushchich & Shtelen, 1983; Mathieu, 1985). In the numerical aspects, various numerical schemes have been proposed and analyzed, including finite difference time domain methods (Bao *et al.*, 2016; Feng & Yin, 2022), exponential wave integrator Fourier pseudospectral method (Bao *et al.*, 2016; Feng *et al.*, 2022) and time-splitting Fourier pseudospectral (TSFP) method (De Frutos & Sanz-Serna, 1989; Fillion-Gourdeau *et al.*, 2012; Bao *et al.*, 2020). However, for the NLDE (1.12) with $0 < \varepsilon \ll 1$, it is interesting to study the long-time dynamics for $t \in [0, T_\varepsilon]$ with $T_\varepsilon = O(1/\varepsilon^2)$. To the best of our knowledge, there are very few numerical analysis results on the error bounds of numerical methods for the long-time dynamics of the NLDE (1.12) in the literature. Recently, we rigorously carried out the error bounds for the long-time dynamics of the Dirac equation with small potentials (Bao *et al.*, 2022b; Feng & Yin, 2022; Feng *et al.*, 2022). Based on the results for the linear case, the TSFP method performs much better than other numerical methods, with the improved uniform error bounds established in the long-time regime by employing the **regularity compensation oscillation** (RCO) technique (Bao *et al.*, 2022b). The aim of this paper is to establish improved uniform bounds on time-splitting methods for the NLDE (1.12) up to the time at $O(1/\varepsilon^2)$. Then, we combine the Fourier pseudospectral method in space and extend the improved uniform error bounds to the full-discretization. With the help of the RCO technique, the improved uniform error bounds are at $O(\varepsilon^2\tau^2 + \tau_0^{m-1})$ and $O(h^{m-1} + \varepsilon^2\tau^2 + \tau_0^{m-1})$, respectively, for the second-order semidiscretization and full-discretization for the NLDE with $O(\varepsilon^2)$-nonlinearity up to the time at $O(1/\varepsilon^2)$, with $m \geqslant 3$ depending on the regularity of the exact solution and $\tau_0 \in (0, 1)$ a fixed chosen parameter. Specifically, when the exact solution is smooth, the improved uniform error bounds are at $O(\varepsilon^2\tau^2)$ and $O(h^{m-1} + \varepsilon^2\tau^2)$ for the second-order semidiscretization and full-discretization, respectively. In contrast with the previous results by standard error estimates in the literature, they are indeed better (or improved) than the uniform error bounds at $O(\tau^2)$ and $O(h^{m-1} + \tau^2)$ up to the time at $O(1/\varepsilon^2)$ for the second-order time-splitting semidiscretization and full-discretization, respectively, especially when $0 < \varepsilon \ll 1$. Moreover, the improved uniform error bounds are extended to the discrete energy of the TSFP method at $O(h^{m-1} + \varepsilon^2\tau^2)$ up to the time at $O(1/\varepsilon^2)$.

The main idea of the RCO technique is to choose the frequency cut-off parameter $\tau_0$ and control high frequency modes ($> 1/\tau_0$) by the regularity of the exact solution, and analyze low frequency modes by phase cancellation and energy method. Similar to the (nonlinear) Schrödinger equation on an irrational rectangle and the nonlinear Klein-Gordon equation as nonperiodic examples in

Bao *et al.* (2022a, 2023), the free Dirac operator is also nonperiodic in 1D. The RCO technique is, not only applicable to the periodic evolutionary PDE, but also to the nonperiodic case.

The rest of this paper is organized as follows. In Section 2, we discretize the NLDE (1.12) in time by the Strang splitting method to obtain the semidiscretization and combine the Fourier pseudospectral method in space for the full-discretization. In Section 3, we establish improved uniform error bounds up to the time at $O(1/\varepsilon^2)$ for the semidiscretization and full-discretization, respectively. In Section 4, we present some numerical results to confirm our error estimates and discuss the improved error bounds for an oscillatory NLDE. Finally, some conclusions are drawn in Section 5. Throughout this paper, we adopt the notation $A \lesssim B$ to represent that there exists a generic constant $C > 0$, which is independent of the mesh size $h$ and time step $\tau$, as well as the parameter $\varepsilon$ such that $|A| \leqslant CB$.

## 2. Discretizations

In this section, we apply a second-order time-splitting method to discretize the NLDE (1.12) and combine the Fourier pseudospectral method in space to derive the TSFP method. For simplicity of notations, we only present the numerical methods and their analysis in 1D, i.e., $d = 1$. Numerical schemes and corresponding results can be easily generalized to the NLDE (1.12) in 2D and to the four-component NLDE (1.9) in 3D. In 1D, the NLDE (1.12) on the computational domain $\Omega = (a, b)$ with periodic boundary conditions collapses to

$$i\partial_t \Phi = \left(-i\sigma_1 \partial_x + \sigma_3\right) \Phi + \varepsilon^2 \mathbf{F}(\Phi)\Phi, \quad x \in \Omega, \quad t > 0, \tag{2.1}$$

$$\Phi(t, a) = \Phi(t, b), \quad t \geqslant 0; \quad \Phi(0, x) = \Phi_0(x), \quad x \in \overline{\Omega}, \tag{2.2}$$

where $\Phi := \Phi(t, x)$, $\Phi_0(a) = \Phi_0(b)$ and the nonlinearity $\mathbf{F}(\Phi)$ is given in (1.13).

For an integer $m \geqslant 0$, we denote by $H^m(\Omega)$ the set of functions $u(x) \in L^2(\Omega)$ with finite $H^m$-norm given by

$$\|u\|_{H^m}^2 = \sum_{l\in\mathbb{Z}} \left(1 + \mu_l^2\right)^m \left|\widehat{u}_l\right|^2, \quad \text{for} \quad u(x) = \sum_{l\in\mathbb{Z}} \widehat{u}_l\, e^{i\mu_l(x-a)}, \quad \mu_l = \frac{2\pi l}{b-a}, \tag{2.3}$$

where $\widehat{u}_l (l \in \mathbb{Z})$ are the Fourier coefficients of the function $u(x)$ (Shen *et al.*, 2011). In fact, the space $H^m(\Omega)$ is the subspace of the classic Sobolev space $W^{m,2}(\Omega)$, which consists of functions with derivatives of order up to $m-1$ being $(b-a)$-periodic.

Denote the index set $\mathcal{T}_M = \{l \mid l = -M/2, -M/2+1, \ldots, M/2-1\}$ and the spaces

$$X_M = \left\{U = (U_0, \ldots, U_M)^T \mid U_j \in \mathbb{C}^2,\ j = 0, 1, \ldots, M,\ U_0 = U_M\right\},$$

$$Y_M = Z_M \times Z_M, \quad Z_M = \operatorname{span}\left\{\phi_l(x) = e^{i\mu_l(x-a)},\ l \in \mathcal{T}_M\right\}.$$

The projection operator $P_M : (L^2(\Omega))^2 \to Y_M$ is defined as

$$(P_M U)(x) := \sum_{l\in\mathcal{T}_M} \widehat{U}_l\, e^{i\mu_l(x-a)}, \quad U(x) \in (L^2(\Omega))^2, \tag{2.4}$$

where

$$\widehat{U}_l = \frac{1}{b-a}\int_a^b U(x)\, e^{-i\mu_l(x-a)}\,\mathrm{d}x, \quad l \in \mathscr{T}_M. \tag{2.5}$$

Define the space $(C_{\mathrm{per}}(\overline{\Omega}))^2 = \{U \in (C(\overline{\Omega}))^2 \mid U(a) = U(b)\}$ and the interpolation operator $I_M : (C_{\mathrm{per}}(\overline{\Omega}))^2 \to Y_M$ or $I_M : X_M \to Y_M$ as

$$(I_M U)(x) := \sum_{l\in\mathscr{T}_M} \widetilde{U}_l\, e^{i\mu_l(x-a)}, \quad U(x) \in (C_{\mathrm{per}}(\overline{\Omega}))^2 \quad \text{or} \quad U \in X_M, \tag{2.6}$$

where

$$\widetilde{U}_l = \frac{1}{M}\sum_{j=0}^{M-1} U_j\, e^{-2ijl\pi/M}, \quad l \in \mathscr{T}_M, \tag{2.7}$$

with $U_j = U(x_j)$ for a function $U(x)$.

### 2.1 *Semidiscretization by a second-order time-splitting method*

Denote the free Dirac operator as

$$\mathbf{T} := -i\sigma_1\partial_x + \sigma_3, \tag{2.8}$$

then the NLDE (2.1) can be expressed as

$$i\partial_t \Phi(t,x) = \mathbf{T}\Phi(t,x) + \varepsilon^2 \mathbf{F}(\Phi(t,x))\Phi(t,x), \quad x \in \Omega, \quad t > 0. \tag{2.9}$$

Choose the time step size as $\tau = \Delta t > 0$ and time steps $t_n = n\tau$ for $n = 0, 1, \ldots$. Denote by $\Phi^{[n]} := \Phi^{[n]}(x)$ the approximation of $\Phi(t_n, x)$ for $n \geqslant 0$, then a semidiscretization for the NLDE (2.1) via the second-order time-splitting (Strang splitting) could be expressed as (Strang, 1968; Lubich, 2008; Bao *et al.*, 2016, 2021b)

$$\Phi^{[n+1]} = \mathscr{S}_\tau\left(\Phi^{[n]}\right) := e^{-\frac{i\tau}{2}\mathbf{T}} e^{-i\varepsilon^2\tau\mathbf{F}\left(e^{-\frac{i\tau}{2}\mathbf{T}}\Phi^{[n]}\right)} e^{-\frac{i\tau}{2}\mathbf{T}}\Phi^{[n]}, \quad n = 0, 1, \ldots, \tag{2.10}$$

with the initial data taken as $\Phi^{[0]} = \Phi_0(x)$ for $x \in \overline{\Omega}$.

REMARK 2.1 The second-order time-splitting (Strang splitting) method is applied to discretize the NLDE (2.1) in time and it is straightforward to design the first-order Lie–Trotter splitting (Trotter, 1959) and higher order schemes, e.g., the fourth-order partitioned Runge–Kutta (PRK4) splitting method (McLachlan & Quispel, 2002; Bao & Yin, 2019).

### 2.2 *Full-discretization*

Given a spatial mesh size $h = (b-a)/M$ with $M$ an even positive integer, the spatial grid points are $x_j := a + jh$ for $j = 0, 1, \ldots, M$. Let $\Phi_j^n$ be the numerical approximation of $\Phi(t_n, x_j)$ and denote

$\Phi^n = (\Phi_0^n, \Phi_1^n, \ldots, \Phi_M^n)^T \in X_M$ as the solution vector at $t = t_n$. The initial data is taken as $\Phi_j^0 = \Phi_0(x_j)$ for $j = 0, 1, \ldots, M$, then from time $t = t_n$ to $t = t_{n+1}$, the TSFP method for discretizing the NLDE (2.1) is given as

$$\begin{aligned}
\Phi_j^{(1)} &= \sum_{l\in\mathcal{T}_M} e^{-i\frac{\tau\Gamma_l}{2}}\widetilde{(\Phi^n)}_l\, e^{i\mu_l(x_j-a)} = \sum_{l\in\mathcal{T}_M} Q_l\, e^{-i\frac{\tau D_l}{2}}(Q_l)^T\widetilde{(\Phi^n)}_l\, e^{\frac{2ijl\pi}{M}},\\
\Phi_j^{(2)} &= e^{-i\varepsilon^2\tau\mathbf{F}\left(\Phi_j^{(1)}\right)}\Phi_j^{(1)} = e^{-i\varepsilon^2\tau\Lambda_j}\Phi_j^{(1)}, \quad 0\leqslant j\leqslant M, \quad n\geqslant 0,\\
\Phi_j^{n+1} &= \sum_{l\in\mathcal{T}_M} e^{-i\frac{\tau\Gamma_l}{2}}\widetilde{(\Phi^{(2)})}_l\, e^{i\mu_l(x_j-a)} = \sum_{l\in\mathcal{T}_M} Q_l\, e^{-i\frac{\tau D_l}{2}}(Q_l)^T\widetilde{(\Phi^{(2)})}_l\, e^{\frac{2ijl\pi}{M}},
\end{aligned} \tag{2.11}$$

where $\Gamma_l = \mu_l\sigma_1 + \sigma_3 = Q_l D_l (Q_l)^T$ with $\delta_l = \sqrt{1+\mu_l^2}$,

$$\Gamma_l = \begin{pmatrix} 1 & \mu_l \\ \mu_l & -1 \end{pmatrix}, \quad Q_l = \begin{pmatrix} \frac{1+\delta_l}{\sqrt{2\delta_l(1+\delta_l)}} & -\frac{\mu_l}{\sqrt{2\delta_l(1+\delta_l)}} \\ \frac{\mu_l}{\sqrt{2\delta_l(1+\delta_l)}} & \frac{1+\delta_l}{\sqrt{2\delta_l(1+\delta_l)}} \end{pmatrix}, \quad D_l = \begin{pmatrix} \delta_l & 0 \\ 0 & -\delta_l \end{pmatrix}, \tag{2.12}$$

and $\Lambda_j = \mathrm{diag}(\Lambda_{j,+}, \Lambda_{j,-})$ with $\Lambda_{j,\pm} = \lambda_2\left|\Phi_j^{(1)}\right|^2 \pm \lambda_1\left(\Phi_j^{(1)}\right)^*\sigma_3\Phi_j^{(1)}$.

## 3. Improved uniform error bounds

In this section, we rigorously prove the improved uniform error bounds for the second-order time-splitting method in propagating the NLDE with $O(\varepsilon^2)$ nonlinearity up to the long-time at $O(1/\varepsilon^2)$. For the simplicity of presentation, we shall assume $\lambda_1 = 0$ in the subsequent discussion, where the results and the proof are also valid if $\lambda_1 \neq 0$ by using the same arguments.

### 3.1 *Main results*

We assume the exact solution $\Phi(t,x)$ of the NLDE (2.1) up to the time at $T_\varepsilon = T/\varepsilon^2$ with $T > 0$ fixed satisfies

(A) $$\Phi \in L^\infty([0,T_\varepsilon];(H^m(\Omega))^2), \quad m\geqslant 3.$$

Let $\Phi^{[n]}$ be the approximation obtained from the time-splitting method (2.10) and $\lambda_1 = 0$ in (1.13). According to the standard analysis in Bao *et al.* (2016), under the assumption (A), for sufficiently small $0 < \tau \leqslant \tau_c$ with $\tau_c > 0$ a constant, there exists a constant $\overline{M} > 0$ depending on $T$ and $\|\Phi\|_{L^\infty([0,T_\varepsilon];(H^m)^2)}$ such that

$$\left\|\Phi^{[n]}\right\|_{H^1} \leqslant \overline{M}, \quad \left\|I_M\Phi^n\right\|_{H^1} \leqslant \overline{M}, \quad 0\leqslant n\leqslant \frac{T/\varepsilon^2}{\tau}. \tag{3.1}$$

In this work, we will establish the following improved uniform error bounds up to the long-time $T_\varepsilon$.

THEOREM 3.1 Under the assumption (A), for $0 < \tau_0 < 1$ sufficiently small and independent of $\varepsilon$ such that, when $0 < \tau \leqslant \alpha \frac{\pi(b-a)\tau_0}{2\sqrt{\tau_0^2(b-a)^2+4\pi^2(1+\tau_0^2)}}$ for a fixed constant $\alpha \in (0,1)$, we have the following improved uniform error bound for any $\varepsilon \in (0,1]$

$$\left\| \Phi(t_n,x) - \Phi^{[n]} \right\|_{H^1} \lesssim \varepsilon^2\tau^2 + \tau_0^{m-1}, \quad 0 \leqslant n \leqslant \frac{T/\varepsilon^2}{\tau}. \tag{3.2}$$

In particular, if the exact solution is sufficiently smooth, e.g., $\Phi(t,x) \in (H^\infty(\Omega))^2$, the last term $\tau_0^{m-1}$ decays exponentially fast and could be ignored practically for small enough $\tau_0$, and the improve uniform error bound would become

$$\left\| \Phi(t_n,x) - \Phi^{[n]} \right\|_{H^1} \lesssim \varepsilon^2\tau^2, \quad 0 \leqslant n \leqslant \frac{T/\varepsilon^2}{\tau}. \tag{3.3}$$

Let $\Phi^n$ be the numerical approximation obtained from the TSFP (2.11), then we have the following improved uniform error bounds for the full-discretization.

THEOREM 3.2 Under the assumption (A), there exist $h_0 > 0$ and $0 < \tau_0 < 1$ sufficiently small and independent of $\varepsilon$ such that, for any $0 < \varepsilon \leqslant 1$, when $0 < h \leqslant h_0$ and $0 < \tau \leqslant \alpha \frac{\pi(b-a)\tau_0}{2\sqrt{\tau_0^2(b-a)^2+4\pi^2(1+\tau_0^2)}}$ for a fixed constant $\alpha \in (0,1)$, the following improved uniform error bound holds

$$\left\| \Phi(t_n,x) - I_M\Phi^n \right\|_{H^1} \lesssim h^{m-1} + \varepsilon^2\tau^2 + \tau_0^{m-1}, \quad 0 \leqslant n \leqslant \frac{T/\varepsilon^2}{\tau}. \tag{3.4}$$

Similarly, for the sufficiently smooth exact solution, e.g., $\Phi(t,x) \in (H^\infty(\Omega))^2$, the improve uniform error bound would become

$$\left\| \Phi(t_n,x) - I_M\Phi^n \right\|_{H^1} \lesssim h^{m-1} + \varepsilon^2\tau^2, \quad 0 \leqslant n \leqslant \frac{T/\varepsilon^2}{\tau}. \tag{3.5}$$

REMARK 3.3 Here, we prove $H^1$-error bounds for 1D problem to control the nonlinearity since $H^1(\mathbb{R})$ is an algebra. Corresponding error estimates should be in $H^2$-norm for 2D and 3D cases (2D case in the sense of (1.12), and 3D case in the sense of the four-component NLDE given in Bao *et al.*, 2016). Of course, higher regularity assumptions of the exact solution are required for higher order Sobolev norm estimates.

REMARK 3.4 Under appropriate assumptions of the exact solution, the improved uniform error bounds could be extended to the first-order Lie–Trotter splitting and the fourth-order PRK splitting method with improved uniform error bounds at $\varepsilon^2\tau$ and $\varepsilon^2\tau^4$, respectively.

REMARK 3.5 For the NLDE (2.1) with general matrix nonlinearity $\mathbf{F}(\Phi)$ in (1.13) when $\lambda_1 \neq 0$, the proof is similar and we omit the details here for brevity.

REMARK 3.6 Define the discrete energy at $t = t_n$ with the mesh size $h$ as

$$E_h^n = h\sum_{j=0}^{M-1}\left[-i\left(\Phi_j^n\right)^*\sigma_1(\Phi')_j^n + \left(\Phi_j^n\right)^*\sigma_3\Phi_j^n + \varepsilon^2 G\left(\Phi_j^n\right)\right], \tag{3.6}$$

where

$$(\Phi')_j^n = i \sum_{l\in\mathscr{T}_M} \mu_l \widetilde{(\Phi^n)}_l \, e^{i\mu_l(x_j-a)}, \quad j = 0, 1, \ldots, M-1, \tag{3.7}$$

then we have the following estimate for the discrete energy

$$\left|E_h^n - E_h^0\right| \lesssim h^{m-1} + \varepsilon^2\tau^2 + \tau_0^{m-1}, \quad 0 \leqslant n \leqslant \frac{T/\varepsilon^2}{\tau}. \tag{3.8}$$

Similarly, for the sufficiently smooth exact solution, e.g., $\Phi(t,x) \in (H^\infty(\Omega))^2$, the estimate for the discrete energy would become

$$\left|E_h^n - E_h^0\right| \lesssim h^{m-1} + \varepsilon^2\tau^2, \quad 0 \leqslant n \leqslant \frac{T/\varepsilon^2}{\tau}. \tag{3.9}$$

### 3.2 *Proof for Theorem* 3.1

For the simplicity of notation, we shall write $\Phi(t_n) := \Phi(t_n, x)$ for $x \in \Omega$ in the proof. Denote the exact solution flow $\Phi(t_n) \to \Phi(t_{n+1})$ as

$$\Phi(t_{n+1}) = \mathscr{S}_{e,\tau}(\Phi(t_n)), \quad 0 \leqslant n \leqslant \frac{T/\varepsilon^2}{\tau}. \tag{3.10}$$

We begin with the local truncation error that is generated by one time step computed via (2.10). By Taylor expansion, we have

$$\begin{aligned}\mathscr{S}_\tau(\Phi(t_n)) = {} & e^{-i\tau\mathbf{T}}\Phi(t_n) - i\varepsilon^2\tau e^{-\frac{i\tau}{2}\mathbf{T}}\left(\mathbf{F}\left(e^{-\frac{i\tau}{2}\mathbf{T}}\Phi(t_n)\right)e^{-\frac{i\tau}{2}\mathbf{T}}\Phi(t_n)\right)\\ & - \varepsilon^4\tau^2\int_0^1 (1-\theta)\, e^{-\frac{i\tau}{2}\mathbf{T}} e^{-i\theta\tau\mathbf{F}\left(e^{-\frac{i\tau}{2}\mathbf{T}}\Phi(t_n)\right)}\left(\mathbf{F}\left(e^{-\frac{i\tau}{2}\mathbf{T}}\Phi(t_n)\right)\right)^2 e^{-\frac{i\tau}{2}\mathbf{T}}\Phi(t_n)\,\mathrm{d}\theta.\end{aligned}$$

On the other hand, by repeatedly using Duhamel's principle (variation-of-constants formula), we can write the exact solution $\Phi(t_{n+1})$ as

$$\begin{aligned}\Phi(t_{n+1}) &= e^{-i\tau\mathbf{T}}\Phi(t_n) - i\varepsilon^2\int_0^\tau e^{-i(\tau-s)\mathbf{T}}\left(\mathbf{F}(\Phi(t_n+s))\Phi(t_n+s)\right)\mathrm{d}s\\ &= e^{-i\tau\mathbf{T}}\Phi(t_n) - i\varepsilon^2\int_0^\tau e^{-i(\tau-s)\mathbf{T}}\left(\mathbf{F}(\Phi(t_n+s))\, e^{-is\mathbf{T}}\Phi(t_n)\right)\mathrm{d}s\\ &\quad - \varepsilon^4\int_0^\tau\int_0^s e^{-i(\tau-s)\mathbf{T}}\mathbf{F}(\Phi(t_n+s))\left(e^{-i(s-\omega)\mathbf{T}}\mathbf{F}(\Phi(t_n+\omega))\Phi(t_n+\omega)\right)\mathrm{d}\omega\,\mathrm{d}s.\end{aligned}$$

Denote

$$f_s(\Phi(t_n)) = e^{-i(\tau-s)\mathbf{T}}\left(\mathbf{F}(\Phi(t_n+s))\, e^{-is\mathbf{T}}\Phi(t_n)\right), \tag{3.11}$$

$$B_{s,\omega}(\Phi(t_n)) = e^{-i(\tau-s)\mathbf{T}}\mathbf{F}(\Phi(t_n+s))\, e^{-i(s-\omega)\mathbf{T}}\mathbf{F}(\Phi(t_n+\omega))\, e^{-i\omega\mathbf{T}}\Phi(t_n), \tag{3.12}$$

then we have the following estimates for the local truncation error.

LEMMA 3.7 For $0 < \varepsilon \leqslant 1$, the local truncation error for the discrete-in-time second-order splitting (2.10) can be written as

$$\begin{aligned}\mathscr{E}^n &:= \mathscr{S}_\tau(\Phi(t_n)) - \Phi(t_{n+1})\\ &= \mathscr{F}(\Phi(t_n)) + \varepsilon^4\left[\int_0^\tau\int_0^s B_{s,\omega}(\Phi(t_n))\,\mathrm{d}\omega\,\mathrm{d}s - \frac{\tau^2}{2}B_{\tau/2,\tau/2}(\Phi(t_n))\right] + \varepsilon^2\mathscr{R}_1^n + \varepsilon^4\mathscr{R}_2^n + \varepsilon^4\mathscr{R}_3^n,\end{aligned}$$

where

$$\mathscr{F}(\Phi(t_n)) = i\varepsilon^2\left(\int_0^\tau f_s(\Phi(t_n))\,\mathrm{d}s - \tau f_{\tau/2}(\Phi(t_n))\right),$$

$$\mathscr{R}_1^n = i\tau e^{-\frac{i\tau}{2}\mathbf{T}}\left[\mathbf{F}(\Phi(t_n+\tau/2)) - \mathbf{F}\left(e^{-\frac{i\tau}{2}\mathbf{T}}\Phi(t_n)\right)\right]e^{-\frac{i\tau}{2}\mathbf{T}}\Phi(t_n),$$

$$\mathscr{R}_2^n = \frac{\tau^2}{2}B_{\tau/2,\tau/2}(\Phi(t_n)) - \tau^2\int_0^1(1-\theta)\, e^{-\frac{i\tau}{2}\mathbf{T}}e^{-i\theta\tau\mathbf{F}\left(e^{-\frac{i\tau}{2}\mathbf{T}}\Phi(t_n)\right)}\left(\mathbf{F}\left(e^{-\frac{i\tau}{2}\mathbf{T}}\Phi(t_n)\right)\right)^2 e^{-\frac{i\tau}{2}\mathbf{T}}\Phi(t_n)\,\mathrm{d}\theta,$$

$$\mathscr{R}_3^n = \int_0^\tau\int_0^s e^{-i(\tau-s)\mathbf{T}}\mathbf{F}(\Phi(t_n+s))\left(e^{-i(s-\omega)\mathbf{T}}\mathbf{F}(\Phi(t_n+\omega))\Phi(t_n+\omega)\right) - B_{s,\omega}(\Phi(t_n))\,\mathrm{d}\omega\,\mathrm{d}s.$$

Under the assumption (A), the following error bounds hold

$$\left\|\mathscr{F}(\Phi(t_n))\right\|_{H^1} \lesssim \varepsilon^2\tau^3, \quad \left\|\mathscr{R}_1^n\right\|_{H^1} \lesssim \varepsilon^2\tau^3, \quad \left\|\mathscr{R}_2^n\right\|_{H^1} \lesssim \tau^3, \quad \left\|\mathscr{R}_3^n\right\|_{H^1} \lesssim \tau^3, \tag{3.13}$$

$$\left\|\int_0^\tau\int_0^s B_{s,\omega}(\Phi(t_n))\,\mathrm{d}\omega\,\mathrm{d}s - \frac{\tau^2}{2}B_{\tau/2,\tau/2}(\Phi(t_n))\right\|_{H^1} \lesssim \tau^3. \tag{3.14}$$

*Proof.* We are going to estimate the terms in the local truncation error one-by-one. Express the quadrature error in the second-order Peano form as

$$\int_0^\tau f_s(\Phi(t_n))\,\mathrm{d}s - \tau f_{\tau/2}(\Phi(t_n)) = \tau^3\int_0^1\kappa_2(\theta)\partial_s^2 f_s(\Phi(t_n))|_{s=\theta\tau}\,\mathrm{d}\theta, \quad \kappa_2(\theta) = \frac{1}{2}\min\{\theta^2,(1-\theta)^2\},$$

which implies

$$\left\|\mathscr{F}(\Phi(t_n))\right\|_{H^1} = \varepsilon^2\left\|\int_0^\tau f_s(\Phi(t_n))\,\mathrm{d}s - \tau f_{\tau/2}(\Phi(t_n))\right\|_{H^1} \lesssim \varepsilon^2\tau^3. \tag{3.15}$$

By Duhamel's principle and Taylor expansion, we have

$$\begin{aligned}\Phi(t_n+\tau/2) &= e^{-\frac{i\tau}{2}\mathbf{T}}\Phi(t_n) - i\varepsilon^2\int_0^{\frac{\tau}{2}} e^{-i(\tau/2-s)\mathbf{T}}\mathbf{F}(\Phi(t_n+s))\Phi(t_n+s)\,\mathrm{d}s\\ &= e^{-\frac{i\tau}{2}\mathbf{T}}\Phi(t_n) - i\varepsilon^2\left(\frac{\tau}{2}\,e^{-\frac{i\tau}{2}\mathbf{T}}\mathbf{F}(\Phi(t_n))\Phi(t_n) + O\left(\partial_s(\mathbf{F}(\Phi(t_n+s))\Phi(t_n+s))\tau^2\right)\right).\end{aligned}$$

With a direct computation and the definition of the nonlinearity $\mathbf{F}(\Phi)$, we have

$$\left\|\mathbf{F}(\Phi(t_n+\tau/2)) - \mathbf{F}\left(e^{-\frac{i\tau}{2}\mathbf{T}}\Phi(t_n)\right)\right\|_{W^{1,\infty}} \lesssim \varepsilon^2\tau^2,$$

which immediately implies $\left\|\mathscr{R}_1^n\right\|_{H^1} \lesssim \varepsilon^2\tau^3$. Similarly, we can prove $\left\|\mathscr{R}_2^n\right\|_{H^1} \lesssim \tau^3$.

Moreover, the quadrature rule implies

$$\begin{aligned}&\left\|\int_0^\tau\int_0^s B_{s,\omega}(\Phi(t_n))\,\mathrm{d}\omega\,\mathrm{d}s - \frac{\tau^2}{2}B_{\tau/2,\tau/2}(\Phi(t_n))\right\|_{H^1}\\ &\quad\lesssim \tau^3\max_{0\leqslant\omega\leqslant s\leqslant\tau}\left(\left\|\partial_s B_{s,\omega}(\Phi(t_n))\right\|_{H^1} + \left\|\partial_\omega B_{s,\omega}(\Phi(t_n))\right\|_{H^1}\right) \lesssim \tau^3,\end{aligned}$$

and

$$\left\|\mathscr{R}_3^n\right\|_{H^1} \lesssim \tau^3\max_{0\leqslant\omega\leqslant s\leqslant\tau}\left\|\,e^{-i(\tau-s)\mathbf{T}}\mathbf{F}(\Phi(t_n+s))\left(e^{-i(s-\omega)\mathbf{T}}\mathbf{F}(\Phi(t_n+\omega))\partial_\omega\Phi(t_n+\omega)\right)\right\|_{H^1} \lesssim \tau^3.$$

Combining above estimates, we complete the proof of Lemma 3.7. □

Now, we are ready to prove Theorem 3.1. Under the assumption (A), the nonlinearity could be controlled by the estimates (3.1) for the numerical solution $\Phi^{[n]}$. Introducing the error function

$$\mathbf{e}^{[n]} := \mathbf{e}^{[n]}(x) = \Phi^{[n]} - \Phi(t_n), \quad n = 0, 1, \ldots, \tag{3.16}$$

we have the error equation as

$$\mathbf{e}^{[n+1]} = \mathscr{S}_\tau(\Phi^{[n]}) - \mathscr{S}_\tau(\Phi(t_n)) + \mathscr{E}^n = e^{-i\tau\mathbf{T}}\mathbf{e}^{[n]} + W^n + \mathscr{E}^n, \quad n \geqslant 0, \tag{3.17}$$

where $W^n := W^n(x)$ is given by

$$W^n(x) = e^{-\frac{i\tau}{2}\mathbf{T}}\left[\left(e^{-i\varepsilon^2\tau\mathbf{F}\left(e^{-\frac{i\tau}{2}\mathbf{T}}\Phi^{[n]}\right)} - I_2\right)e^{-\frac{i\tau}{2}\mathbf{T}}\Phi^{[n]} - \left(e^{-i\varepsilon^2\tau\mathbf{F}\left(e^{-\frac{i\tau}{2}\mathbf{T}}\Phi(t_n)\right)} - I_2\right)e^{-\frac{i\tau}{2}\mathbf{T}}\Phi(t_n)\right],$$

with the bound implied by (3.1)

$$\left\|W^n(x)\right\|_{H^1} \lesssim \varepsilon^2\tau\left\|\mathbf{e}^{[n]}\right\|_{H^1}. \tag{3.18}$$

Based on (3.17), we obtain

$$\mathbf{e}^{[n+1]} = e^{-i(n+1)\tau\mathbf{T}}\mathbf{e}^{[0]} + \sum_{k=0}^{n} e^{-i(n-k)\tau\mathbf{T}}\left(W^k + \mathscr{E}^k\right), \quad 0 \leqslant n \leqslant \frac{T/\varepsilon^2}{\tau} - 1. \tag{3.19}$$

Noticing $\mathbf{e}^{[0]} = \mathbf{0}$, combining (3.13), (3.14) and (3.18), we have the estimates for $0 \leqslant n \leqslant T_\varepsilon/\tau - 1$,

$$\left\|\mathbf{e}^{[n+1]}\right\|_{H^1} \lesssim \varepsilon^2\tau^2 + \varepsilon^2\tau\sum_{k=0}^{n}\left\|\mathbf{e}^{[k]}\right\|_{H^1} + \left\|\sum_{k=0}^{n} e^{-i(n-k)\tau\mathbf{T}}\mathscr{F}(\Phi(t_k))\right\|_{H^1}. \tag{3.20}$$

In order to obtain the improved uniform error bounds (3.2), we will employ the RCO technique (Bao *et al.*, 2022a, 2023) to deal with the last term on the RHS of (3.20). From the NLDE (2.1), we find that $\partial_t\Phi + i\mathbf{T}\Phi = O(\varepsilon^2)$. It is natural to consider the 'twisted variable'

$$\Psi(t,x) = e^{it\mathbf{T}}\Phi(t,x), \quad t \geqslant 0, \tag{3.21}$$

which satisfies the equation $\partial_t\Psi(t,x) = \varepsilon^2 e^{it\mathbf{T}}\left(\mathbf{F}\left(e^{-it\mathbf{T}}\Psi(t,x)\right)e^{-it\mathbf{T}}\Psi(t,x)\right)$. Under the assumption (A), we have $\|\Psi\|_{L^\infty([0,T_\varepsilon];(H^m(\Omega))^2)} \lesssim 1$ and $\|\partial_t\Psi\|_{L^\infty([0,T_\varepsilon];(H^m(\Omega))^2)} \lesssim \varepsilon^2$ with

$$\left\|\Psi(t_{n+1}) - \Psi(t_n)\right\|_{H^m} \lesssim \varepsilon^2\tau, \quad 0 \leqslant n \leqslant \frac{T/\varepsilon^2}{\tau} - 1. \tag{3.22}$$

**Step 1**. Choose the cut-off parameter on the Fourier modes. Let $\tau_0 \in (0,1)$ and $M_0 = 2\lceil 1/\tau_0\rceil \in \mathbb{Z}^+$ ($\lceil\cdot\rceil$ is the ceiling function) with $1/\tau_0 \leqslant M_0/2 < 1 + 1/\tau_0$. Under the assumption (A), we have the following estimate

$$\left\|P_{M_0}\mathscr{F}\left(e^{-it_k\mathbf{T}}P_{M_0}\Psi(t_k)\right) - \mathscr{F}\left(e^{-it_k\mathbf{T}}\Psi(t_k)\right)\right\|_{H^1} \lesssim \varepsilon^2\tau\tau_0^{m-1}. \tag{3.23}$$

Based on above estimates, (3.20) would imply for $0 \leqslant n \leqslant T_\varepsilon/\tau - 1$,

$$\left\|\mathbf{e}^{[n+1]}\right\|_{H^1} \lesssim \tau_0^{m-1} + \varepsilon^2\tau^2 + \varepsilon^2\tau\sum_{k=0}^{n}\left\|\mathbf{e}^{[k]}\right\|_{H^1} + \left\|\mathscr{L}^n\right\|_{H^1}, \tag{3.24}$$

with

$$\mathscr{L}^n = \sum_{k=0}^{n} e^{i(k+1)\tau\mathbf{T}}P_{M_0}\mathscr{F}\left(e^{-ik\tau\mathbf{T}}\left(P_{M_0}\Psi(t_k)\right)\right). \tag{3.25}$$

**Step 2**. Analyze the low Fourier modes term $\mathscr{L}^n$. For $l \in \mathscr{T}_{M_0}$, define the index set $\mathscr{I}_l^{M_0}$ associated to $l$ as

$$\mathscr{I}_l^{M_0} = \left\{(l_1,l_2,l_3) \mid l_1 - l_2 + l_3 = l,\ l_1,l_2,l_3 \in \mathscr{T}_{M_0}\right\}. \tag{3.26}$$

We introduce

$$\Pi_l^+ = Q_l \mathrm{diag}(1,0)(Q_l)^T, \quad \Pi_l^- = Q_l \mathrm{diag}(0,1)(Q_l)^T, \tag{3.27}$$

where $\Pi_l^\pm$ are the projectors onto the eigenspaces of $\Gamma_l$ corresponding to the eigenvalues $\pm\delta_l$, respectively. Moreover, we have $(\Pi_l^\pm)^T = \Pi_l^\pm$, $\Pi_l^+ + \Pi_l^- = I_2$, $(\Pi_l^\pm)^2 = \Pi_l^\pm$, $\Pi_l^\pm \Pi_l^\mp = \mathbf{0}$. By direct computation, we have

$$e^{it\mathbf{T}} P_{M_0} \Psi(t_k) = \sum_{l \in \mathscr{T}_{M_0}} \left( e^{it\delta_l} \Pi_l^+ + e^{-it\delta_l} \Pi_l^- \right) \widehat{\Psi}_l(t_k)\, e^{i\mu_l(x-a)}. \tag{3.28}$$

In view of the definition of $\mathscr{F}$ in Lemma 3.7, we have the following expansion

$$e^{i(k+1)\tau\mathbf{T}} P_{M_0} \left( f_s \left( e^{-ik\tau\mathbf{T}} P_{M_0} \Psi(t_k) \right) \right) = \lambda_2 \sum_{l \in \mathscr{T}_{M_0}} \sum_{(l_1,l_2,l_3) \in \mathscr{I}_l^{M_0}} \sum_{\nu_j = \pm, j=1,2,3,4} \mathscr{G}_{k,l,l_1,l_2,l_3}^{\nu_1,\nu_2,\nu_3,\nu_4}(s)\, e^{i\mu_l(x-a)},$$

where the coefficients $\mathscr{G}_{k,l,l_1,l_2,l_3}^{\nu_1,\nu_2,\nu_3,\nu_4}(s)$ are functions of $s$ defined as

$$\mathscr{G}_{k,l,l_1,l_2,l_3}^{\nu_1,\nu_2,\nu_3,\nu_4}(s) = e^{i(t_k+s)\delta_{l,l_1,l_2,l_3}^{\nu_1,\nu_2,\nu_3,\nu_4}} \Pi_l^{\nu_1} \left( \widehat{\Psi}_{l_2}(t_k) \right)^* \Pi_{l_2}^{\nu_3} \Pi_{l_1}^{\nu_2} \widehat{\Psi}_{l_1}(t_k) \Pi_{l_3}^{\nu_4} \widehat{\Psi}_{l_3}(t_k) \tag{3.29}$$

with $\delta_{l,l_1,l_2,l_3}^{\nu_1,\nu_2,\nu_3,\nu_4} = \nu_1\delta_l - \nu_2\delta_{l_1} + \nu_3\delta_{l_2} - \nu_4\delta_{l_3}$. Thus, we have

$$\mathscr{L}^n = \lambda_2 i\varepsilon^2 \sum_{k=0}^{n} \sum_{l \in \mathscr{T}_{M_0}} \sum_{(l_1,l_2,l_3) \in \mathscr{I}_l^{M_0}} \sum_{\nu_j = \pm, j=1,2,3,4} \Upsilon_{k,l,l_1,l_2,l_3}^{\nu_1,\nu_2,\nu_3,\nu_4}\, e^{i\mu_l(x-a)}, \tag{3.30}$$

where

$$\Upsilon_{k,l,l_1,l_2,l_3}^{\nu_1,\nu_2,\nu_3,\nu_4} = -\tau \mathscr{G}_{k,l,l_1,l_2,l_3}^{\nu_1,\nu_2,\nu_3,\nu_4}(\tau/2) + \int_0^\tau \mathscr{G}_{k,l,l_1,l_2,l_3}^{\nu_1,\nu_2,\nu_3,\nu_4}(s)\, \mathrm{d}s = r_{l,l_1,l_2,l_3}^{\nu_1,\nu_2,\nu_3,\nu_4}\, e^{it_k \delta_{l,l_1,l_2,l_3}^{\nu_1,\nu_2,\nu_3,\nu_4}} c_{k,l,l_1,l_2,l_3}^{\nu_1,\nu_2,\nu_3,\nu_4}, \tag{3.31}$$

and the vector coefficients $c_{l,l_1,l_2,l_3}^{\nu_1,\nu_2,\nu_3,\nu_4}$ and the scalar coefficient $r_{l,l_1,l_2,l_3}^{\nu_1,\nu_2,\nu_3,\nu_4}$ are given as

$$c_{l,l_1,l_2,l_3}^{\nu_1,\nu_2,\nu_3,\nu_4} = \Pi_l^{\nu_1} (\widehat{\Psi}_{l_2}(t_k))^* \Pi_{l_2}^{\nu_3} \Pi_{l_1}^{\nu_2} \widehat{\Psi}_{l_1}(t_k) \Pi_{l_3}^{\nu_4} \widehat{\Psi}_{l_3}(t_k), \tag{3.32}$$

$$\begin{aligned} r_{l,l_1,l_2,l_3}^{\nu_1,\nu_2,\nu_3,\nu_4} &= -\tau e^{i\tau\delta_{k,l,l_1,l_2,l_3}^{\nu_1,\nu_2,\nu_3,\nu_4}/2} + \int_0^\tau e^{is\delta_{k,l,l_1,l_2,l_3}^{\nu_1,\nu_2,\nu_3,\nu_4}}\, \mathrm{d}s \\ &= O\left( \tau^3 \left( \delta_{k,l,l_1,l_2,l_3}^{\nu_1,\nu_2,\nu_3,\nu_4} \right)^2 \right). \end{aligned} \tag{3.33}$$

We only need to consider the case $\delta^{\nu_1,\nu_2,\nu_3,\nu_4}_{k,l,l_1,l_2,l_3} \neq 0$ as $r^{\nu_1,\nu_2,\nu_3,\nu_4}_{l,l_1,l_2,l_3} = 0$ if $\delta^{\nu_1,\nu_2,\nu_3,\nu_4}_{k,l,l_1,l_2,l_3} = 0$. For $l \in \mathscr{T}_{M_0}$ and $(l_1,l_2,l_3) \in \mathscr{I}_l^{M_0}$, we have

$$\left|\delta^{\nu_1,\nu_2,\nu_3,\nu_4}_{l,l_1,l_2,l_3}\right| \leqslant 4\delta_{M_0/2} = 4\sqrt{1+\mu^2_{M_0/2}} < 4\sqrt{1+\frac{4\pi^2(1+\tau_0)^2}{\tau_0^2(b-a)^2}}, \tag{3.34}$$

which implies $\frac{\tau}{2}\left|\delta^{\nu_1,\nu_2,\nu_3,\nu_4}_{l,l_1,l_2,l_3}\right| < \alpha\pi$ when $0 < \tau \leqslant \alpha\frac{\pi(b-a)\tau_0}{2\sqrt{\tau_0^2(b-a)^2+4\pi^2(1+\tau_0)^2}} := \tau_0^\alpha$ $(0 < \tau_0, \alpha < 1)$. Since $\mathscr{G}^{\nu_1,\nu_2,\nu_3,\nu_4}_{k,l,l_1,l_2,l_3}$ in (3.29) is similar, it suffices to consider the typical case $\nu_1 = \nu_2 = \nu_3 = \nu_4 = +$. Denoting $S^n_{l,l_1,l_2,l_3} = \sum_{k=0}^n e^{it_k\delta^{+,+,+,+}_{l,l_1,l_2,l_3}}$ $(n \geqslant 0)$, for $0 < \tau < \tau_0^\alpha$, we have

$$\left|S^n_{l,l_1,l_2,l_3}\right| \leqslant \frac{1}{\left|\sin\left(\tau\delta^{+,+,+,+}_{l,l_1,l_2,l_3}/2\right)\right|} \leqslant \frac{C}{\tau\left|\delta^{+,+,+,+}_{l,l_1,l_2,l_3}\right|}, \quad \forall n \geq 0, \tag{3.35}$$

with $C = \frac{2\alpha\pi}{\sin(\alpha\pi)}$. Using summation-by-parts, we find from (3.31) that

$$\sum_{k=0}^n \Upsilon^{+,+,+,+}_{k,l,l_1,l_2,l_3} = r^{+,+,+,+}_{l,l_1,l_2,l_3,l_4}\left[\sum_{k=0}^{n-1} S^k_{l,l_1,l_2,l_3}\left(c^{+,+,+,+}_{k,l,l_1,l_2,l_3} - c^{+,+,+,+}_{k+1,l,l_1,l_2,l_3}\right) + S^n_{l,l_1,l_2,l_3}c^{+,+,+,+}_{n,l,l_1,l_2,l_3}\right], \tag{3.36}$$

with

$$\begin{aligned} c^{+,+,+,+}_{k,l,l_1,l_2,l_3} - c^{+,+,+,+}_{k+1,l,l_1,l_2,l_3} &= \Pi_l^+\left(\left(\widehat{\Psi}_{l_2}(t_k)\right)^*\Pi_{l_2}^+\Pi_{l_1}^+\left(\widehat{\Psi}_{l_1}(t_k) - \widehat{\Psi}_{l_1}(t_{k+1})\right)\right)\Pi_{l_3}^+\widehat{\Psi}_{l_3}(t_k) \\ &\quad + \Pi_l^+\left(\widehat{\Psi}_{l_2}(t_k) - \widehat{\Psi}_{l_2}(t_{k+1})\right)^*\Pi_{l_2}^+\Pi_{l_1}^+\widehat{\Psi}_{l_1}(t_{k+1})\Pi_{l_3}^+\widehat{\Psi}_{l_3}(t_k) \\ &\quad + \Pi_l^+\left(\widehat{\Psi}_{l_2}(t_{k+1})\right)^*\Pi_{l_2}^+\Pi_{l_1}^+\widehat{\Psi}_{l_1}(t_{k+1})\Pi_{l_3}^+\left(\widehat{\Psi}_{l_3}(t_k) - \widehat{\Psi}_{l_3}(t_{k+1})\right). \end{aligned} \tag{3.37}$$

Combining (3.33), (3.35), (3.36) and (3.37), we have

$$\begin{aligned} \left|\sum_{k=0}^n \Upsilon^{+,+,+,+}_{k,l,l_1,l_2,l_3}\right| &\lesssim \tau^2\left|\delta^{+,+,+,+}_{l,l_1,l_2,l_3}\right|\sum_{k=0}^{n-1}\Big(\left|\widehat{\Psi}_{l_1}(t_k) - \widehat{\Psi}_{l_1}(t_{k+1})\right|\left|\widehat{\Psi}_{l_2}(t_k)\right|\left|\widehat{\Psi}_{l_3}(t_k)\right| \\ &\quad + \left|\widehat{\Psi}_{l_1}(t_{k+1})\right|\left|\widehat{\Psi}_{l_2}(t_k) - \widehat{\Psi}_{l_2}(t_{k+1})\right|\left|\widehat{\Psi}_{l_3}(t_k)\right| \\ &\quad + \left|\widehat{\Psi}_{l_1}(t_{k+1})\right|\left|\widehat{\Psi}_{l_2}(t_{k+1})\right|\left|\widehat{\Psi}_{l_3}(t_k) - \widehat{\Psi}_{l_3}(t_{k+1})\right|\Big) \\ &\quad + \tau^2\left|\delta^{+,+,+,+}_{l,l_1,l_2,l_3}\right|\left|\widehat{\Psi}_{l_1}(t_n)\right|\left|\widehat{\Psi}_{l_2}(t_n)\right|\left|\widehat{\Psi}_{l_3}(t_n)\right|. \end{aligned} \tag{3.38}$$

The same estimates (3.38) above hold for $\sum_{k=0}^{n}\Upsilon_{k,l,l_1,l_2,l_3}^{\pm,\pm,\pm,\pm}$ ($l\in\mathscr{T}_{M_0}$, $(l_1,l_2,l_3)\in\mathscr{T}_l^{M_0}$). For the $H^1$-norm estimates, we notice that for $l\in\mathscr{T}_{M_0}$ and $(l_1,l_2,l_3)\in\mathscr{I}_l^{M_0}$, there holds

$$\left(1+|\mu_l|\right)\left|\delta_{l,l_1,l_2,l_3}^{\nu_1,\nu_2,\nu_3,\nu_4}\right|\lesssim\prod_{j=1}^{3}\left(1+\mu_{l_j}^2\right). \tag{3.39}$$

Based on (3.30), (3.38) and (3.39), we have

$$\begin{aligned}
\left\|\mathscr{L}^n\right\|_{H^1}^2 =&\lambda_2^2\varepsilon^4\sum_{l\in\mathscr{T}_{M_0}}\left(1+\mu_l^2\right)\left|\sum_{(l_1,l_2,l_3)\in\mathscr{I}_l^{M_0}}\sum_{\nu_j=\pm}\sum_{k=0}^{n}\Upsilon_{k,l,l_1,l_2,l_3}^{\nu_1,\nu_2,\nu_3,\nu_4}\right|^2\\
\lesssim&\,\varepsilon^4\tau^4\Bigg\{\sum_{l\in\mathscr{T}_{M_0}}\left(\sum_{(l_1,l_2,l_3)\in\mathscr{I}_l^{M_0}}\left|\widehat{\Psi}_{l_1}(t_n)\right|\left|\widehat{\Psi}_{l_2}(t_n)\right|\left|\widehat{\Psi}_{l_3}(t_n)\right|\prod_{j=1}^{3}(1+\mu_{l_j}^2)\right)^2\\
&+n\sum_{k=1}^{n-1}\Bigg[\sum_{l\in\mathscr{T}_{M_0}}\left(\sum_{(l_1,l_2,l_3)\in\mathscr{I}_l^{M_0}}\left|\widehat{\Psi}_{l_1}(t_k)-\widehat{\Psi}_{l_1}(t_{k+1})\right|\left|\widehat{\Psi}_{l_2}(t_k)\right|\left|\widehat{\Psi}_{l_3}(t_k)\right|\prod_{j=1}^{3}\left(1+\mu_{l_j}^2\right)\right)^2\\
&+\left(\sum_{(l_1,l_2,l_3)\in\mathscr{I}_l^{M_0}}\left|\widehat{\Psi}_{l_1}(t_{k+1})\right|\left|\widehat{\Psi}_{l_2}(t_k)-\widehat{\Psi}_{l_2}(t_{k+1})\right|\left|\widehat{\Psi}_{l_3}(t_k)\right|\prod_{j=1}^{3}\left(1+\mu_{l_j}^2\right)\right)^2\\
&+\left(\sum_{(l_1,l_2,l_3)\in\mathscr{I}_l^{M_0}}\left|\widehat{\Psi}_{l_1}(t_{k+1})\right|\left|\widehat{\Psi}_{l_2}(t_{k+1})\right|\left|\widehat{\Psi}_{l_3}(t_k)-\widehat{\Psi}_{l_3}(t_{k+1})\right|\prod_{j=1}^{3}\left(1+\mu_{l_j}^2\right)\right)^2\Bigg]\Bigg\}.
\end{aligned} \tag{3.40}$$

Introduce the auxiliary function $\Theta(x)=\sum_{l\in\mathbb{Z}}(1+\mu_l^2)\left|\widehat{\Psi}_l(t_n)\right|e^{i\mu_l(x-a)}$, where $\Theta(x)\in H^{m-2}$ implied by assumption (A) and $\|\Theta\|_{H^s}\lesssim\|\Psi(t_n)\|_{H^{s+2}}$ ($s\leqslant m-2$). Expanding

$$|\Theta(x)|^2\Theta(x)=\sum_{l\in\mathbb{Z}}\sum_{l_1-l_2+l_3=l,l_j\in\mathbb{Z}}\prod_{j=1}^{3}\left(\left(1+\mu_{l_j}^2\right)\left|\widehat{\Psi}_{l_j}(t_n)\right|\right)e^{i\mu_l(x-a)},$$

we could obtain that

$$\begin{aligned}
&\sum_{l\in\mathscr{T}_{M_0}}\left(\sum_{(l_1,l_2,l_3)\in\mathscr{I}_l^{M_0}}\left|\widehat{\Psi}_{l_1}(t_n)\right|\left|\widehat{\Psi}_{l_2}(t_n)\right|\left|\widehat{\Psi}_{l_3}(t_n)\right|\prod_{j=1}^{3}\left(1+\mu_{l_j}^2\right)\right)^2\\
&\leqslant\sum_{l\in\mathbb{Z}}\left(\sum_{l_1-l_2+l_3=l,l_j\in\mathbb{Z}}\left|\widehat{\Psi}_{l_1}(t_n)\right|\left|\widehat{\Psi}_{l_2}(t_n)\right|\left|\widehat{\Psi}_{l_3}(t_n)\right|\prod_{j=1}^{3}\left(1+\mu_{l_j}^2\right)\right)^2\\
&=\left\||\Theta(x)|^2\Theta(x)\right\|_{L^2}^2\lesssim\|\Theta(x)\|_{H^1}^6\lesssim\|\Psi(t_n)\|_{H^3}^6\lesssim 1.
\end{aligned} \tag{3.41}$$

Thus, in light of (3.22), we could obtain the estimate for each term in (3.25) similarly as

$$\left\|\mathscr{L}^n\right\|_{H^1}^2 \lesssim \varepsilon^4\tau^4\left[\|\Psi(t_k)\|_{H^3}^6 + n\sum_{k=1}^{n-1}\|\Psi(t_k)-\Psi(t_{k+1})\|_{H^3}^2(\|\Psi(t_k)\|_{H^3}+\|\Psi(t_{k+1})\|_{H^3})^4\right]$$

$$\lesssim \varepsilon^4\tau^4 + n\varepsilon^4\tau^4(\varepsilon^2\tau)^2 \lesssim \varepsilon^4\tau^4, \quad 0\leqslant n\leqslant \frac{T/\varepsilon^2}{\tau}-1. \tag{3.42}$$

Finally, combining (3.24) and (3.42), we have

$$\|\mathbf{e}^{[n+1]}\|_{H^1} \lesssim \tau_0^{m-1} + \varepsilon^2\tau^2 + \varepsilon^2\tau\sum_{k=0}^{n}\|\mathbf{e}^{[k]}\|_{H^1}, \quad 0\leqslant n\leqslant \frac{T/\varepsilon^2}{\tau}-1. \tag{3.43}$$

Discrete Gronwall inequality would yield

$$\|\mathbf{e}^{[n+1]}\|_{H^1} \lesssim \tau_0^{m-1} + \varepsilon^2\tau^2, \quad 0\leqslant n\leqslant \frac{T/\varepsilon^2}{\tau}-1, \tag{3.44}$$

and the improved uniform error bound (3.2) in Theorem 3.1 holds.

### 3.3 *Proof for Theorem* 3.2

Before the proof of the improved estimate (3.4) for the fully discrete scheme (2.11), we have the following observations. Previous work on establishing the error estimates for the splitting scheme was mainly based on the error splitting approach, i.e., to estimate the semidiscrete-in-time error (3.2), and the difference between $\Phi^{[n]}(\cdot)$ and $\Phi^n$. To maintain the full convergence order $h^m$ in space, we need the bound of $\|\Phi^{[n]}\|_{H^m}$, which is generally not available under the assumption (A) for arbitrary $T>0$ in the nonlinear case. Following the classical arguments of Gronwall type, we can show $\|\Phi^{[n]}\|_{H^m}$ is bounded for certain $n\tau\leqslant T_0/\varepsilon^2$, and $T_0>0$ is determined by $\|\Phi_0\|_{H^m}$ only, which is not suitable to derive the estimates over the whole interval $[0,T/\varepsilon^2]$ in the assumption (A). Another typical approach is to use the error estimates to control the $\|\Phi^{[n]}\|_{H^{m-2}}$ (or $\|\Phi^{[n]}\|_{H^{m-1}}$ by the first order estimates) following Theorem 3.1, which would yield a sub-optimal $H^1$ estimate in space as $h^{m-3}$ (or $h^{m-2}$). Here, we shall present a different approach to directly work with the fully discrete scheme (2.11) without the detour via semidiscretization-in-time. Using same notations and similar to the proof of Lemma 3.7, we have the following results for the local truncation error for the TSFP (2.11).

LEMMA 3.8 The local truncation error of the TSFP (2.11) for the NLDE (2.1) can be written as

$$\overline{\mathscr{E}}^n := P_M\mathscr{S}_\tau(P_M\Phi(t_n)) - P_M\Phi(t_{n+1}) = P_M\mathscr{F}(P_M\Phi(t_n)) + \mathscr{Y}^n, \quad 0\leqslant n\leqslant \frac{T/\varepsilon^2}{\tau}-1,$$

where the following error bounds hold under the assumption (A),

$$\left\|\mathscr{F}(P_M\Phi(t_n))\right\|_{H^1} \lesssim \varepsilon^2\tau^3, \quad \left\|\mathscr{Y}^n\right\|_{H^1} \lesssim \varepsilon^4\tau^3 + \varepsilon^2\tau h^{m-1}. \tag{3.45}$$

*Proof.* The proof can be conducted similarly to that for Lemma 3.7 and we omit the details here for brevity. □

We shall establish the error bound (3.4) for the full-discretization (2.11). By the standard Fourier projection and interpolation results, $\left\|\Phi(t_n) - I_M\Phi^n\right\|_{H^1} \lesssim \left\|I_M\Phi^n - P_M\Phi(t_n)\right\|_{H^1} + h^{m-1}$, and it suffices to consider the growth of the error function $\mathbf{e}^n = I_M\Phi^n - P_M\Phi(t_n) \in Y_M$ $(n \geq 0)$. For $0 \leqslant n \leqslant \frac{T/\varepsilon^2}{\tau} - 1$, we have

$$\mathbf{e}^{n+1} = I_M\Phi^{n+1} - P_M\mathscr{S}_\tau(P_M\Phi(t_n)) + \overline{\mathscr{E}}^n = e^{-i\tau\mathbf{T}}\mathbf{e}^n + \mathbf{Z}^n + \overline{\mathscr{E}}^n, \tag{3.46}$$

where $\mathbf{Z}^n \in Y_M$ is given by

$$\mathbf{Z}^n = e^{-\frac{i\tau}{2}\mathbf{T}}\left[I_M\left(\left(e^{-i\varepsilon^2\tau\mathbf{F}\left(e^{-\frac{i\tau}{2}\mathbf{T}}I_M\Phi^n\right)} - I_2\right)e^{-\frac{i\tau}{2}\mathbf{T}}I_M\Phi^n\right)\right.$$
$$\left. - P_M\left(\left(e^{-i\varepsilon^2\tau\mathbf{F}\left(e^{-\frac{i\tau}{2}\mathbf{T}}P_M\Phi(t_n)\right)} - I_2\right)e^{-\frac{i\tau}{2}\mathbf{T}}P_M\Phi(t_n)\right)\right].$$

Under the assumption (A), we shall prove by induction that, there exist two constants $h_c > 0$ and $\tau_c > 0$ such that for $0 < h < h_c$ and $0 < \tau < \tau_c$,

$$\|\mathbf{e}^n\|_{H^1} \leqslant C(h^{m-1} + \tau^2), \quad \|I_M\Phi^n\|_{H^1} \leqslant M + 1, \quad 0 \leqslant n \leqslant \frac{T/\varepsilon^2}{\tau}, \tag{3.47}$$

where $M = \|\Phi\|_{L^\infty([0,T_\varepsilon];(H^1)^2)}$, and $C > 0$ is independent of $n$, $h$, $\varepsilon$ and $\tau$.

For $n = 0$, (3.47) holds for sufficiently small $0 < h < h_1$ $(h_1 > 0)$ by the standard Fourier interpolation results, i.e., $\|\mathbf{e}^0\|_{H^1} \leqslant C_1h^{m-1}$ $(C_1 > 0)$ and $\|I_M\Phi^0\|_{H^1} \leqslant M + 1$.

Assume (3.47) holds for $0 \leqslant n \leqslant p \leqslant \frac{T/\varepsilon^2}{\tau} - 1$ ($C$ to be chosen later), and we consider the case $n = p + 1$. Recalling the definition of $\mathbf{Z}^n$, replacing $P_M$ by $I_M$, using the equivalence between the $H^1$ norm of $I_M\Phi^n$ with its grid version for the finite difference as discussed in the appendix of Bao & Cai (2014), we have the estimates on $\mathbf{Z}^n$ $(n \leqslant p)$ for $0 < h < h_2$ $(h_2 > 0)$ and $0 < \tau < \tau_2$ $(\tau_2 > 0)$,

$$\left\|\mathbf{Z}^n\right\|_{H^1} \leqslant \varepsilon^2\tau\left(C_2h^{m-1} + C_M\|\mathbf{e}^n\|_{H^1}\right), \quad n \leqslant p, \tag{3.48}$$

where $C_2 > 0$ depends on $\|\Phi\|_{L^\infty([0,T_\varepsilon];(H^m)^2)}$ and $C_M$ depends on $M$. From (3.46), we obtain

$$\mathbf{e}^{n+1} = \mathbf{e}^{-i(n+1)\tau\mathbf{T}}\mathbf{e}^0 + \sum_{k=0}^{n}\mathbf{e}^{-i(n-k)\tau\mathbf{T}}\left(\mathbf{Z}^k + \overline{\mathscr{E}}^k\right), \quad 0 \leqslant n \leqslant \frac{T/\varepsilon^2}{\tau} - 1. \tag{3.49}$$

Combining the estimates (3.45) and (3.48), we derive for $0 \leqslant n \leqslant p \leqslant \frac{T/\varepsilon^2}{\tau} - 1$, $0 < h < h_3$ $(h_3 > 0)$ and $0 < \tau < \tau_3$ $(\tau_3 > 0)$

$$\|\mathbf{e}^{n+1}\|_{H^1} \leqslant C_3(h^{m-1} + \tau^2) + C_M\varepsilon^2\tau\sum_{k=0}^{n}\|\mathbf{e}^k\|_{H^1}, \tag{3.50}$$

and the discrete Gronwall inequality implies for $0 < \tau < \tau_4$ ($\tau_4 > 0$),

$$\|\mathbf{e}^{n+1}\|_{H^1} \leqslant C_4(h^{m-1} + \tau^2), \tag{3.51}$$

with $C_4 > 0$ independent of $\varepsilon$, $\tau$, $h$ and $m$. By the Fourier interpolation and projection properties, we have for sufficiently small mesh size and time step size $0 < h < h_4$ ($h_4 > 0$) and $0 < \tau < \tau_5$ ($\tau_5 > 0$),

$$\|I_M\Phi^{p+1}\|_{H^1} \leqslant \|\mathbf{e}^{p+1}\|_{H^1} + \|P_M\Phi(t_{p+1})\|_{H^1} \leqslant C_4(h^{m-1} + \tau^2) + M \leqslant 1 + M. \tag{3.52}$$

By taking $C = \max\{C_1, C_2, C_3, C_4\}$, and choosing $\tau_c = \min\{\tau_1, \tau_2, \tau_3, \tau_4, \tau_5\}$, $h_c = \min\{h_1, h_2, h_3, h_4\}$, we conclude that (3.47) holds for $n = p + 1$. By induction, we obtain the estimates in (3.47) for all $0 \leqslant n \leqslant \frac{T/\varepsilon^2}{\tau}$.

Having established (3.47), we have the control on the nonlinear term $\mathbf{Z}^n$ in (3.48), and we are ready to show the improved error estimates in the fully discrete case. Combining the estimates (3.45) and (3.48), we get for $0 \leqslant n \leqslant \frac{T/\varepsilon^2}{\tau} - 1$,

$$\|\mathbf{e}^{n+1}\|_{H^1} \lesssim h^{m-1} + \varepsilon^2\tau^2 + \varepsilon^2\tau\sum_{k=0}^{n}\|\mathbf{e}^k\|_{H^1} + \left\|\sum_{k=0}^{n} e^{-i(n-k)\tau\mathbf{T}}P_M\mathscr{F}(P_M\Phi(t_k))\right\|_{H^1}, \tag{3.53}$$

where $\mathscr{F}(\cdot)$ is defined in Lemma 3.7. Following the semidiscrete case, we introduce a cut-off parameter $\tau_0 \in (0, 1)$ and $M_0 = 2\lceil 1/\tau_0\rceil \in \mathbb{Z}^+$ ($\lceil\cdot\rceil$ is the ceiling function) with $1/\tau_0 \leqslant M_0/2 < 1 + 1/\tau_0$. Under the assumption (A), replacing $P_M$ by $P_{M_0}$ in (3.53), we can derive

$$\left\|\mathbf{e}^{n+1}\right\|_{H^1} \lesssim h^{m-1} + \tau_0^{m-1} + \varepsilon^2\tau^2 + \varepsilon^2\tau\sum_{k=0}^{n}\left\|\mathbf{e}^k\right\|_{H^1} + \left\|\mathscr{L}^n\right\|_{H^1}, \tag{3.54}$$

where $\mathscr{L}^n$ is defined in (3.25). Recalling the estimate (3.42) for $\mathscr{L}^n$, we obtain

$$\left\|\mathbf{e}^{n+1}\right\|_{H^1} \lesssim h^{m-1} + \tau_0^{m-1} + \varepsilon^2\tau^2 + \varepsilon^2\tau\sum_{k=0}^{n}\left\|\mathbf{e}^k\right\|_{H^1}, \quad 0 \leqslant n \leqslant \frac{T/\varepsilon^2}{\tau} - 1. \tag{3.55}$$

The discrete Gronwall inequality would then yield

$$\left\|\mathbf{e}^{n+1}\right\|_{H^1} \lesssim h^{m-1} + \tau_0^{m-1} + \varepsilon^2\tau^2, \quad 0 \leqslant n \leqslant \frac{T/\varepsilon^2}{\tau} - 1, \tag{3.56}$$

which completes the proof for the error bound (3.4).

## 4. Numerical results and extensions

In this section, we present some numerical results of the TSFP method for solving the NLDE (1.12) in terms of the mesh size $h$, time step $\tau$ and the parameter $0 < \varepsilon \leqslant 1$ to illustrate our improved uniform error bounds.

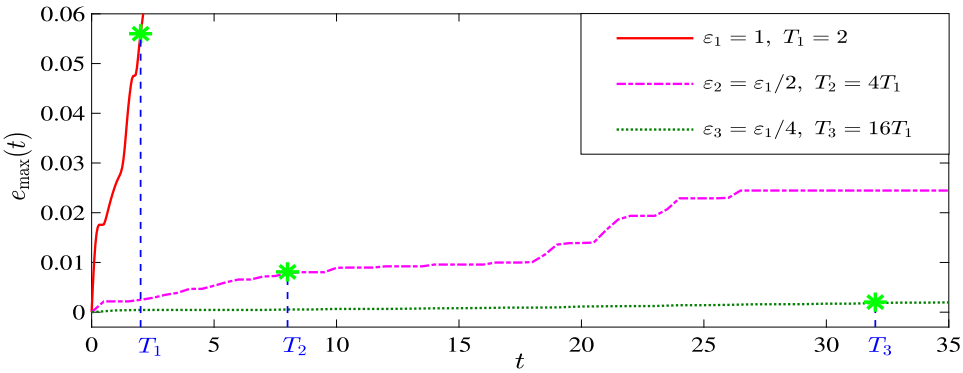


FIG. 1. Long-time temporal errors for the wave function of the TSFP method for the NLDE (1.12) in 1D with different $\varepsilon$. Stars on each line refer to the errors at the long time $T_j = T_1/\varepsilon_j^2$ for $j = 1, 2, 3$.

### 4.1 *The long-time dynamics in 1D*

To test the accuracy, we choose the initial data as

$$\phi_1(0,x) = \frac{2}{2+\sin^2(x)}, \quad \phi_2(0,x) = \frac{2}{1+\sin^2(x)}, \quad x \in (0, 2\pi). \tag{4.1}$$

Since the exact solution is unknown, we use the TSFP method with a very small time step $\tau_e = 10^{-4}$ and a fine mesh size $h_e = \pi/64$ to generate the 'reference' solution numerically. Let $\Phi^n = (\Phi_0^n, \Phi_1^n, \ldots, \Phi_M^n)^T$ be the numerical solution obtained by the TSFP method with a given mesh size $h$, time step $\tau$ and the parameter $\varepsilon$ at time $t = t_n$, then we introduce the discrete $H^1$-error of the wave function as

$$e(t_n) = \|\Phi^n - \Phi(t_n,\cdot)\|_{H^1} = \sqrt{h\sum_{j=0}^{M-1}\left|\Phi_j^n - \Phi(t_n,x_j)\right|^2 + h\sum_{j=0}^{M-1}\left|(\Phi')_j^n - \Phi'(t_n,x_j)\right|^2},$$

where $(\Phi')_j^n$ is defined in (3.7).

For the long-time dynamics, we quantify the errors as $e_{\max}(t_n) = \max_{0\leqslant q\leqslant n} e(t_q)$. In the rest of the paper, the spatial mesh size is always chosen sufficiently small such that the spatial errors can be neglected when considering the long-time temporal errors.

Figure 1 displays the long-time errors of the TSFP method (2.11) for the NLDE (1.12) in 1D with fixed time step size $\tau$ and different $\varepsilon$. Stars on each line refer to the errors at the long time $T_j = T_1/\varepsilon_j^2$ for $j = 1, 2, 3$, and the long-time error up to the time at $O(1/\varepsilon^2)$ becomes quarter when $\varepsilon$ is half, which verifies that the improved uniform error bounds behave like $O(\varepsilon^2)$ for fixed time step size $\tau$. In addition, Fig. 2 and Fig. 3 show the spatial and temporal errors of the TSFP methods for the NLDE (1.12) in 1D at $t = 1/\varepsilon^2$, respectively. Figure 2 indicates the spectral accuracy of the TSFP method in space and the spatial errors are independent of the parameter $\varepsilon$. From Fig. 3(a), we observe the second-order convergence of the TSFP method in time for the fixed $\varepsilon$. Figure 3(b) again validates that the long-time

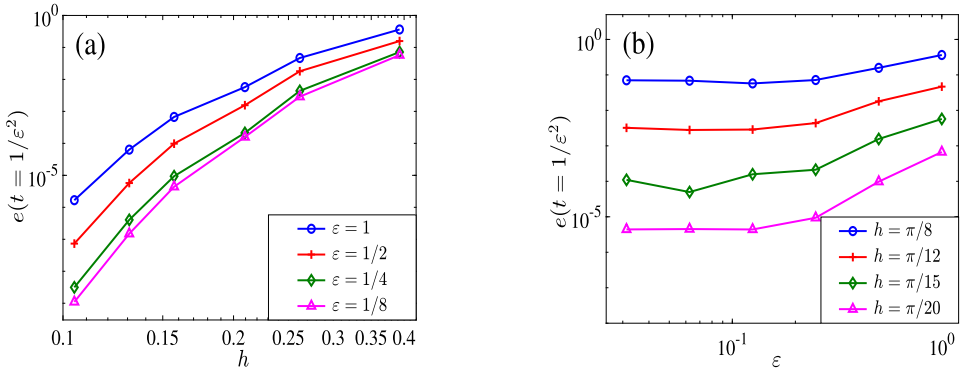


FIG. 2. Long-time spatial errors of the TSFP method for the NLDE (1.12) in 1D at $t = 1/\varepsilon^2$.

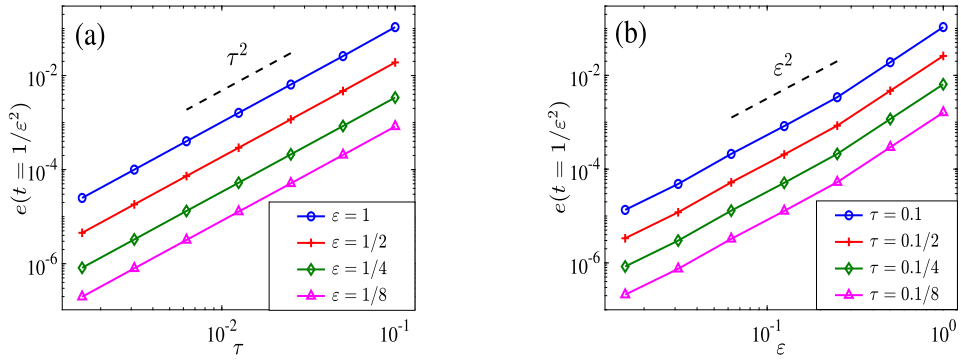


FIG. 3. Long-time temporal errors of the TSFP method for the NLDE (1.12) in 1D at $t = 1/\varepsilon^2$.

errors behave like $O(\varepsilon^2\tau^2)$ up to the time at $O(1/\varepsilon^2)$. Figure 4 shows the error of the discrete energy $E_h^n$ also behaves like $O(\varepsilon^2\tau^2)$ up to the time at $O(1/\varepsilon^2)$.

### 4.2 *The long-time dynamics in 2D*

In this subsection, we show an example in 2D with the irrational aspect ratio of the domain $(x, y) \in (0, 2\pi) \times (0, 1)$. In the numerical experiment, we choose the initial data as

$$\phi_1(0, x) = \sin(2x) + \sin(2\pi y), \quad \phi_2(0, x) = \frac{1}{1 + \cos^2(2x)} + \cos(2\pi y). \tag{4.2}$$

Figure 5 presents the long-time errors of the TSFP method for the NLDE (1.12) in 2D with fixed time step size $\tau$ and different $\varepsilon$. Stars on each line refer to the errors at the long time $T_j = T_1/\varepsilon_j^2$ for $j = 1, 2, 3$, which confirm the improved uniform error bounds in 2D. Figure 6 plots the temporal errors of the TSFP method for the NLDE in 2D at $t = 1/\varepsilon^2$, which indicates the second-order convergence in time and again validates the improved uniform error bounds at $O(\varepsilon^2\tau^2)$ up to the time at $O(1/\varepsilon^2)$.

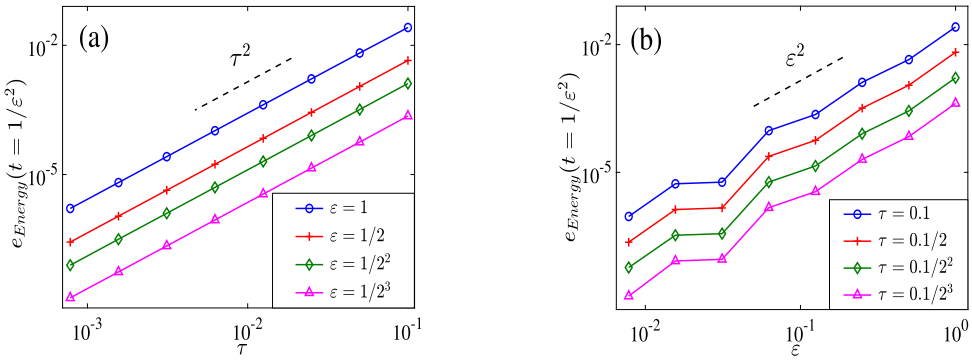


FIG. 4. Long-time error for the discretized energy $E_h^n$ of the TSFP method for the NLDE (1.12) in 1D at $t = 1/\varepsilon^2$.

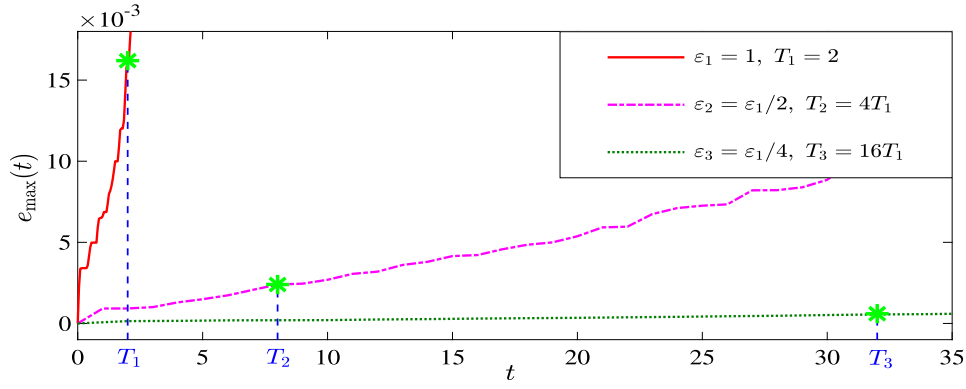


FIG. 5. Long-time temporal errors of the TSFP method for the NLDE (1.12) in 2D with different. $\varepsilon$ Stars on each line refer to the errors at the long time $T_j = T_1/\varepsilon_j^2$ for $j = 1, 2, 3$.

### 4.3 *Extension to the oscillatory NLDE*

In this subsection, we extend the TSFP method and error estimates to an oscillatory NLDE, which propagates waves with wave length at $O(\varepsilon^2)$ in time and wave speed at $O(\varepsilon^{-2})$ in space. Introduce a re-scale in time $s = \varepsilon^2 t$ and $\widetilde{\Phi}(s, \mathbf{x}) = \Phi(t, \mathbf{x})$, then the NLDE (1.12) could be reformulated into the following oscillatory NLDE

$$i\partial_s \widetilde{\Phi} = \frac{1}{\varepsilon^2}\left[-i\sum_{j=1}^{d}\sigma_j\partial_j + \sigma_3\right]\widetilde{\Phi} + \mathbf{F}(\widetilde{\Phi})\widetilde{\Phi} \quad x \in \Omega, \quad t > 0, \tag{4.3}$$

with the initial data

$$\widetilde{\Phi}(s = 0, \mathbf{x}) = \widetilde{\Phi}_0(\mathbf{x}) = O(1), \quad \mathbf{x} \in \overline{\Omega}. \tag{4.4}$$

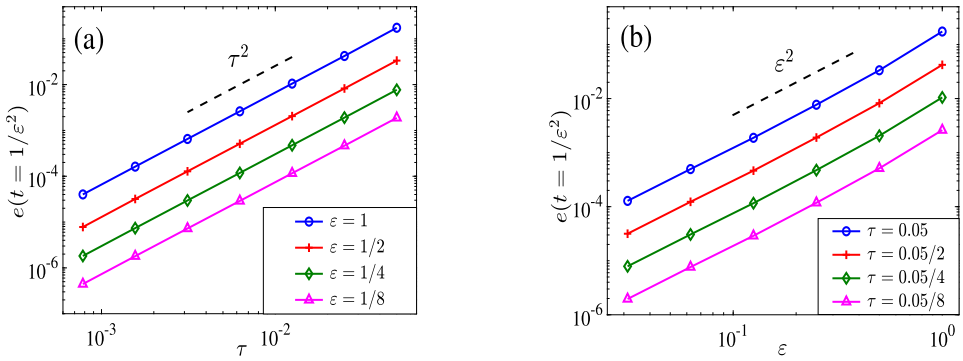


FIG. 6. Long-time temporal errors of the TSFP method for the NLDE (1.12) in 2D at $t = 1/\varepsilon^2$.

The solution of the oscillatory NLDE (4.3) propagates waves with amplitude at $O(1)$, wavelength at $O(1)$ and $O(\varepsilon^2)$ in space and time, respectively, and wave speed at $O(\varepsilon^{-2})$ in space. We remark here the oscillatory nature of the NLDE (4.3) is quite different from the NLDE in the nonrelativistic limit regime, which has been widely studied in Hunziker (1975), Bao *et al.* (2016), Lemou *et al.* (2017), Cai & Wang (2019) and Krämer *et al.* (2021). In fact, in this regime, the wave speed is at $O(1/\varepsilon^2)$, while the NLDE in the nonrelativistic limit regime propagates waves with wave speed at $O(1)$. According to the time rescaling, by taking the time step $\kappa = \varepsilon^2\tau$, we could extend the improved error bounds on the TSFP method for the long-time problem to the oscillatory NLDE (4.3) up to the fixed time $T$. We also just present the result in 1D and it is straightforward to extend to 2D and 3D cases.

THEOREM 4.1 Let $\widetilde{\Phi}^n$ be the numerical approximation obtained from the TSFP method for the oscillatory NLDE (4.3) in 1D. Assume the exact solution $\widetilde{\Phi}(s,x)$ satisfies

$$\widetilde{\Phi}(s,x) \in L^\infty([0,T];(H^m(\Omega))^2), \quad m \geqslant 3,$$

then there exist $h_0 > 0$ and $0 < \kappa_0 < 1$ sufficiently small and independent of $\varepsilon$ such that for any $0 < \varepsilon \leqslant 1$, when $0 < h \leqslant h_0$ and $0 < \kappa \leqslant \varepsilon^2\alpha\kappa_0$ for a fixed constant $\alpha \in (0,1)$, the following improved uniform error bound holds

$$\left\|\widetilde{\Phi}(s_n,x) - I_M\widetilde{\Phi}^n\right\|_{H^1} \lesssim h^{m-1} + \frac{\kappa^2}{\varepsilon^2} + \kappa_0^{m-1}, \quad 0 \leqslant n \leqslant \frac{T}{\kappa}. \tag{4.5}$$

In particular, if the exact solution is sufficiently smooth, e.g., $\widetilde{\Phi}(t,x) \in (H^\infty)^2$, the improved uniform error bound for small $\kappa_0$ would become

$$\left\|\widetilde{\Phi}(s_n,x) - I_M\widetilde{\Phi}^n\right\|_{H^1} \lesssim h^{m-1} + \frac{\kappa^2}{\varepsilon^2}, \quad 0 \leqslant n \leqslant \frac{T}{\kappa}. \tag{4.6}$$

The proof of the improved error bounds for the oscillatory NLDE (4.3) in Theorem 4.1 is quite similar to the long-time problem. We omit the details here for brevity and present some numerical results to

TABLE 2 *Temporal errors of the TSFP method for the NLDE (4.3) in 1D at $t = 1$*

| $e(t=1)$ | $\kappa_0 = 0.05$ | $\kappa_0/4$ | $\kappa_0/4^2$ | $\kappa_0/4^3$ | $\kappa_0/4^4$ |
|---|---|---|---|---|---|
| $\varepsilon_0 = 1$ | **1.26E−2** | 7.57E−4 | 4.72E−5 | 2.95E−6 | 1.84E−7 |
| order | **–** | 2.03 | 2.00 | 2.00 | 2.00 |
| $\varepsilon_0/2$ | 1.21E−1 | **5.71E−3** | 3.52E−4 | 2.20E−5 | 1.37E−6 |
| order | – | **2.20** | 2.01 | 2.00 | 2.00 |
| $\varepsilon_0/2^2$ | 5.39E−2 | 9.18E−3 | **3.85E−4** | 2.37E−5 | 1.48E−6 |
| order | – | 1.23 | **2.29** | 2.01 | 2.00 |
| $\varepsilon_0/2^3$ | 2.40E−1 | 1.08E−2 | 2.13E−3 | **8.68E−5** | 5.34E−6 |
| order | - | 2.24 | 1.17 | **2.31** | 2.01 |
| $\varepsilon_0/2^4$ | 1.17E−1 | 3.80E−2 | 2.46E−3 | 6.76E−4 | **2.46E−5** |
| order | – | 0.81 | 1.97 | 0.93 | **2.39** |

The bold entries stand for the $\varepsilon$ dependent step sizes satisfying $\kappa = O(\varepsilon^2)$.

confirm the sharpness of the improved error bounds. The initial data is chosen as

$$\widetilde{\phi}_1(0,x) = 4x^4(1-x)^4 + 2, \quad \widetilde{\phi}_2(0,x) = 4x^4(1-x)^4, \quad x \in (0,1). \tag{4.7}$$

The regularity is enough to ensure the improved error bounds.

Table 2 lists the temporal errors of the TSFP method for the oscillatory NLDE (4.3) in 1D with different $\varepsilon$. It can be clearly observed that the second-order convergence can only be observed when $\kappa \lesssim \varepsilon^2$ (cf. the upper triangle above the diagonal with bold letters) and the temporal errors behave like $O(\kappa^2/\varepsilon^2)$. Along each diagonal in the table, i.e., with $\kappa = O(\varepsilon^2)$, we observe linear convergence with respect to $\kappa$, which confirms the error bound at $\frac{\kappa^2}{\varepsilon^2} = O\left(\frac{\kappa^2}{\kappa}\right) = O(\kappa)$ in (4.1).

## 5. Conclusions

Improved uniform error bounds on time-splitting methods for the long-time dynamics of the weakly NLDE were rigorously proven. With the help of the RCO technique, the long-time errors up to the time at $O(1/\varepsilon^2)$ for the semidiscretization and full-discretization are at $O(\varepsilon^2\tau^2)$ and $O(h^{m-1} + \varepsilon^2\tau^2)$, respectively, which improve the standard error bounds in the literature at $O(\tau^2)$ and $O(h^{m-1} + \tau^2)$ for the semidiscretization and full-discretization, respectively, especially when $0 < \varepsilon \ll 1$. The improved error bounds were extended to an oscillatory NLDE up to a fixed time $T$. Numerical results in 1D and 2D agreed well with the theoretical results and suggested that the error bounds are sharp.

## Funding

Ministry of Education of Singapore (MOE-T2EP20122-0002 (A-8000962-00-00) to W.B. and Y.F.); Natural Science Foundation of China (12171041 and 11771036 to Y.C.). Part of the work was done when the authors were visiting the Institute for Mathematical Sciences at the National University of Singapore in February 2023.

## References


Balabane, M., Cazenave, T., Douady, A. & Merle, F. (1988) Existence of excited states for a nonlinear Dirac field. *Commun. Math. Phys.*, **119**, 153–176.

Bao, W. & Cai, Y. (2014) Uniform and optimal error estimates of an exponential wave integrator sine pseudospectral method for the nonlinear Schrödinger equation with wave operator. *SIAM J. Numer. Anal.*, **52**, 1103–1127.

Bao, W., Cai, Y. & Feng, Y. (2022a) Improved uniform error bounds on time-splitting methods for long-time dynamics of the nonlinear Klein–Gordon equation with weak nonlinearity. *SIAM J. Numer. Anal.*, **60**, 1962–1984.

Bao, W., Cai, Y. & Feng, Y. (2023) Improved uniform error bounds of the time-splitting methods for the long-time (nonlinear) Schrödinger equation. *Math. Comp.* **91**, 1109–1139.

Bao, W., Cai, Y., Jia, X. & Tang, Q. (2017) Numerical methods and comparison for the Dirac equation in the nonrelativistic limit regime. *J. Sci. Comput.*, **71**, 1094–1134.

Bao, W., Cai, Y., Jia, X. & Yin, J. (2016) Error estimates of numerical methods for the nonlinear Dirac equation in the nonrelativistic limit regime. *Sci. China Math.*, **59**, 1461–1494.

Bao, W., Cai, Y. & Yin, J. (2020) Super-resolution of time-splitting methods for the Dirac equation in the nonrelativistic regime. *Math. Comp.*, **89**, 2141–2173.

Bao, W., Cai, Y. & Yin, J. (2021) Uniform error bounds of time-splitting methods for the nonlinear Dirac equation in the nonrelativistic regime without magnetic potential. *SIAM J. Numer. Anal.*, **59**, 1040–1066.

Bao, W., Feng, Y. & Yin, J. (2022b) Improved uniform error bounds on time-splitting methods for the long-time dynamics of the Dirac equation with small potentials. *Multiscale Model. Simul.*, **20**, 1040–1062.

Bao, W. & Yin, J. (2019) A fourth-order compact time-splitting Fourier pseudospectral method for the Dirac equation. *Res. Math. Sci.*, **6**, article 11.

Bartsch, T. & Ding, Y. (2006) Solutions of nonlinear Dirac equations. *J. Differential Equations*, **226**, 210–249.

Brinkman, D., Heitzinger, C. & Markowich, P. A. (2014) A convergent 2D finite-difference scheme for the Dirac–Poisson system and the simulation of graphene. *J. Comput. Phys.*, **257**, 318–332.

Cai, Y. & Wang, Y. (2019) Uniformly accurate nested Picard iterative integrators for the Dirac equation in the nonrelativistic limit regime. *SIAM J. Numer. Anal.*, **57**, 1602–1624.

Cazenave, T. & Vazquez, L. (1986) Existence of localized solutions for a classical nonlinear Dirac field. *Commun. Math. Phys.*, **105**, 35–47.

Chang, S. J., Ellis, S. D. & Lee, B. W. (1975) Chiral confinement: an exact solution of the massive Thirring model. *Phys. Rev. D*, **11**, 3572–3582.

De Frutos, J. & Sanz-Serna, J. M. (1989) Split-step spectral schemes for nonlinear Dirac systems. *J. Comput. Phys.*, **83**, 407–423.

Dirac, P. A. M. (1928) The quantum theory of the electron. *Proc. R. Soc. Lond. A*, **117**, 610–624.

Dirac, P. A. M. (1958) *Principles of Quantum Mechanics,* vol. 11. London: Oxford University Press.

Esteban, M. J. & Séré, E. (1997) Existence and multiplicity of solutions for linear and nonlinear Dirac problems. *Partial Differential Equations and Their Applications (Toronto, ON, 1995), CRM Proc. Lecture Notes,* vol. 12. Amer. Math. Soc., Providence, RI, 107–118.

Faou, E. & Grébert, B. (2011) Hamiltonian interpolation of splitting approximations for nonlinear PDEs. *Found. Comput. Math.*, **11**, 381–415.

Faou, E., Grébert, B. & Paturel, E. (2010) Birkhoff normal form for splitting methods applied to semilinear Hamiltonian PDEs. Part II. Abstract splitting. *Numer. Math.*, **114**, 459–490.

Fefferman, C. L. & Weistein, M. I. (2012) Honeycomb lattice potentials and Dirac points. *J. Amer. Math. Soc.*, **25**, 1169–1220.

Feng, Y., Xu, Z. & Yin, J. (2022) Uniform error bounds of exponential wave integrator methods for the long-time dynamics of the Dirac equation with small potentials. *Appl. Numer. Math.*, **172**, 50–66.

Feng, Y. & Yin, J. (2022) Spatial resolution of different discretizations over long-time for the Dirac equation with small potentials. *J. Comput. Appl. Math.*, **412**, 114342.

Fillion-Gourdeau, F., Lorin, E. & Bandrauk, A. D. (2012) Numerical solution of the time-dependent Dirac equation in coordinate space without fermion-doubling. *Comput. Phys. Commun.*, **183**, 1403–1415.
Fushchich, W. I. & Shtelen, W. M. (1983) On some exact solutions of the nonlinear Dirac equation. *J. Phys. A: Math Gen.*, **16**, 271–277.
Fushchich, W. I. & Zhdanov, R. Z. (1989) Symmetry and exact solutions of nonlinear spinor equations. *Phys. Rep.*, **172**, 123–174.
Gauckler, L. & Lubich, C. (2010) Splitting integrators for nonlinear Schrödinger equations over long times. *Found. Comput. Math.*, **10**, 275–302.
Haddad, L. H. & Carr, L. D. (2009) The nonlinear Dirac equation in Bose–Einstein condensates: foundation and symmetries. *Phys. D*, **238**, 1413–1421.
Haddad, L. H. & Carr, L. D. (2015) The nonlinear Dirac equation in Bose–Einstein condensates: superfluid fluctuations and emergent theories from relativistic linear stability equations. *New J. Phys.*, **17**, 093037.
Hairer, E. & Lubich, C. (2008) Spectral semi-discretisations of weakly nonlinear wave equations over long times. *Found. Comput. Math.*, **8**, 319–334.
Hunziker, W. (1975) On the nonrelativistic limit of the Dirac theory. *Commun. Math. Phys.*, **40**, 215–222.
Komech, A. & Komech, A. (2010) Global attraction to solitary waves for a nonlinear Dirac equation with mean field interaction. *SIAM J. Math. Anal.*, **42**, 2944–2964.
Krämer, P., Schratz, K. & Zhao, X. (2021) Splitting methods for nonlinear Dirac equations with Thirring type interaction in the nonrelativistic limit regime. *J. Comput. Appl. Math.*, **387**, 112494.
Lemou, M., Méhats, F. & Zhao, X. (2017) Uniformly accurate numerical schemes for the nonlinear Dirac equation in the nonrelativistic limit regime. *Commun. Math. Sci.*, **15**, 1107–1128.
Lubich, C. (2008) On splitting methods for Schrödinger–Poisson and cubic nonlinear Schrödinger equations. *Math. Comp.*, **77**, 2141–2153.
Mathieu, P. (1985) Soliton solutions for Dirac equations with homogeneous non-linearity in (1+1) dimensions. *J. Phys. A: Math. Gen.*, **18**, L1061–L1066.
McLachlan, R. I. & Quispel, G. R. W. (2002) Splitting methods. *Acta Numer.*, **11**, 341–434.
Pecher, H. (2014) Local well-posedness for the nonlinear Dirac equation in two space dimensions. *Commun. Pure Appl. Anal.*, **13**, 673–685.
Rafelski, J. (1977) Soliton solutions of a selfinteracting Dirac field in three space dimensions. *Phys. Lett. B*, **66**, 262–266.
Sasaki, H. (2015) Small data scattering for the one-dimensional nonlinear Dirac equation with power nonlinearity. *Commun. Partial Differential Equations*, **40**, 1959–2004.
Shen, J., Tang, T. & Wang, L.-L. (2011) *Spectral Methods: Algorithms, Analysis and Applications*. Berlin, Heidelberg: Springer.
Soler, M. (1970) Classical, stable, nonlinear spinor field with positive rest energy. *Phys. Rev. D*, **1**, 2766–2769.
Strang, G. (1968) On the construction and comparison of difference schemes. *SIAM J. Numer. Anal.*, **5**, 505–517.
Takahashi, K. (1979) Soliton solutions of nonlinear Dirac equations. *J. Math. Phys.*, **20**, 1232–1238.
Thirring, W. E. (1958) A soluble relativistic field theory. *Ann. Phys.*, **3**, 91–112.
Trotter, H. F. (1959) On the product of semi-groups of operators. *Proc. Amer. Math. Soc.*, **10**, 545–551.